Genetic control of plasticity in root morphology and anatomy of rice in response to water deficit

Kadam, N. N., Tamilselvan, A., Lawas, L. M. F., Quinones, C., Bahuguna, R. N., Thomson, M. J., ... Jagadish, K. S. V.

Plant Physiology Preview. Published on June 9, 2017, as DOI:10.1104/pp.17.00500

Running Title– Genetic control of rice root morphology and anatomy

Research area – Eco-physiology and Sustainability

Title: Genetic control of plasticity in root morphology and anatomy of rice in response to water-deficit

Authors - Niteen N Kadam[1,2], Anandhan Tamilselvan[1,3], Lovely M F Lawas[1], Cherryl Quinones[1], Rajeev N Bahuguna[1], Michael J Thomson[1,4], Michael Dingkuhn[1], Raveendran Muthurajan[3], Paul C Struik[2], Xinyou Yin[2*], Krishna S V Jagadish[1,5*]

Affiliations

[1]International Rice Research Institute (IRRI), DAPO, Box 7777, Metro Manila, Philippines

[2]Centre for Crop Systems Analysis, Department of Plant Sciences, Wageningen University & Research, PO Box 430, 6700 AK Wageningen, The Netherlands

[3]Tamil Nadu Agricultural University, Coimbatore, Tamil Nadu, India

[4]Department of Soil and Crop Sciences, Texas A & M University, College Station, Texas, USA

[5]Department of Agronomy, Kansas State University, Manhattan, USA

Summary

The genetic analysis of root morphology and anatomy in a rice diversity panel resulted in identification of the genetic loci that regulates the rooting plasticity in water-deficit.

Author Contributions

X.Y., P.C.S., and K.S.V.J conceived the project and its components; N.N.K., K.S.V.J., X.Y., P.C.S. and R.N.B. implemented the experiment; M.D. performed the genotyping; N.N.K., A.T., L.M.F.L., C.Q., R.M., and R.N.B performed the phenotyping; N.K.K. performed the GWAS including both the conventional and multi locus approach; N.N.K. drafted the figures, tables and manuscript; X.Y., K.S.V.J, and P.C.S. supervised the data processing and the

preparation of the drafts; N.N.K., K.S.V.J., X.Y., P.C.S., M.D., M.J.T. interpreted the data and wrote the final paper.

Corresponding author

Correspondence should be addressed to SVK (k.jagadish@irri.org) and XY (xinyou.yin@wur.nl).

Abstract

Elucidating the genetic control of rooting behaviour under water-deficit stress is essential to breed climate-robust rice cultivars. Using a diverse panel of 274 *indica* genotypes grown under control and water-deficit conditions during vegetative growth, we phenotyped 35 traits, mostly related to root morphology and anatomy, involving ~45,000 root scanning images and nearly ~25,000 cross-sections from the root-shoot junction. Phenotypic plasticity of these traits was quantified as the relative change in trait value under water-deficit compared to control conditions. We then carried out a genome-wide association analysis on these traits and their plasticity, using 45,608 high quality SNPs. One hundred four significant loci were detected for these traits under control condition, 106 were detected under water-deficit stress, and 76 were detected for trait plasticity. We predicted 296 (control), 284 (water-deficit stress) and 233 (plasticity) *a priori* candidate genes within linkage disequilibrium (LD) blocks for these loci. We identified key a *priori* candidate genes regulating root growth and development and relevant alleles that upon validation can help improve rice adaptation to water-deficit stress.

Keywords

Oryza sativa, root plasticity, linkage disequilibrium, loci, *a priori* candidate genes, multi-locus analysis.

Introduction

Increasing water scarcity, caused by global climate change and increasing competition for available water resources, is a major constraint for crop production and global food security (Rosegrant et al., 2009). Rice (*Oryza sativa* L.) is the most important staple cereal. It requires 2-3 times more water than dryland cereals, as it is predominately grown under flooded paddy cultivation. Improving rice adaptation to water-deficit conditions could support developing dryland rice production systems, thereby reducing the dependence of rice on large volumes of water. Therefore, current rice breeding programmes are striving to develop cultivars that are productive under water-deficit conditions (Bernier et al., 2009; Kumar et al., 2014; Sandhu et al., 2014). This will require a suite of morphological, anatomical and physiological adjustments of shoot and root traits (Kadam et al., 2015; Sandhu et al., 2016). Interactions among these traits in response to water-deficit are complex, rendering effective knowledge-intensive breeding strategies.

To adapt to water-deficit stress, rice needs to be plastic. Phenotypic plasticity is a characteristic of a given genotype to produce a distinct phenotype in response to changing environments (Nicotra et al., 2010). Mostly, the plasticity of traits is desirable for better stress adaptation. Both natural and human selection have created many rice types that are sensitive and tolerant to water scarcity and have different levels of (desired or undesirable) plasticity. Climate change and increased water scarcity demand a new compromise among stress resistance, stress escape or avoidance, and potential productivity through phenotypic plasticity. Previous studies have shown the role of root trait plasticity in improving water-deficit stress adaptation. For instance, the plasticity of root-length density in water-deficit stress contributes to rice grain yield stability (Sandhu et al., 2016). Similarly, the comparative analysis between water-deficit tolerant rice and wheat has demonstrated the functional relevance of plasticity in shoot and root traits to better adapt to water-deficit stress (Kadam et

al., 2015). However, phenotypic traits that express constitutively with no plasticity could also provide stress adaptation. For example, changes in the root angle during early development resulted in constitutive expression of deep root architecture that helps in later stages to increase rice grain yield under water-deficit (Uga et al., 2013).

Although phenotypic plasticity is heritable (Nicotra and Davidson, 2010), plasticity *per se* is usually not targeted when breeding rice for water-deficit conditions. Breeding for plasticity in traits other than yield would offer alternative routes to enhance resilience to stress conditions (Sambatti and Caylor, 2007) and to tap into a larger rice genetic diversity pool for adapting to stressful environments (McCouch et al., 2013). Plasticity of traits is controlled by key environment-sensing genes (Juenger, 2013). Yet, no study has been undertaken to comprehensively demonstrate the quantitative variation in root and shoot plasticity and the underlying genetic control using diverse rice genotypes grown under water-deficit stress.

We herein report a genome-wide association study (GWAS) in rice to unravel the genetic control of phenotypic traits in control and water-deficit stress and their plasticity. Given our diverse *indica* rice panel that incorporates more evolutionary recombination events compared with bi-parental mapping populations (Ingvarsson and Street, 2011), we expect to detect phenotype associations with narrow genomic regions or even nearby/within causal genes. Specific objectives were (1) to assess natural genetic variability in root and shoot morphological and anatomical traits in control and water-deficit conditions and their plasticity as a relative change, (2) to associate genetic variation in root and shoot phenotypic plasticity with adaptive significance under water-deficit stress, and (3) to elucidate the genetic architecture of phenotypic traits and their plasticity by identifying the genomic loci with underlying *a priori* candidate genes.

Results and Discussion

Genotypic variation in phenotypic traits and their interrelations

Rice exhibits large functional diversity due to strong natural and human selection pressure, which underlies evolutionary variation in traits inducing stress adaptation (McCouch et al., 2013). A set of 274 rice *indica* genotypes assembled from major rice growing regions across the world was evaluated to assess the variation in phenotypic traits **(Supplementary Figure S1 and Supplementary Dataset S1)**. In total, 35 phenotypic traits, broadly classified into five categories (shoot morphology, whole-plant physiology, root morphology, root anatomy, and dry matter production), were evaluated on plants grown in control and water-deficit stress conditions during the vegetative phase **(Table 1)**.

Genotypic variation observed in all traits across treatments was strong ($P \leq 0.001$), except in root length classes RL3035 and RL35 (**Supplementary Table S1)**. The broad-sense heritability (H^2) ranged from 0.10 to 0.89 in the control and from 0.03 to 0.88 under water-deficit stress (**Supplementary Table S2**). A principal component analysis (PCA) identified 8 significant principal components (PCs) with eigenvalue >1, cumulatively explaining > 80% of the total variation for the 35 traits across the panel in each treatment **(Supplementary Figure S2)**. The first PC, explaining > 35% of the total variation, was associated with genotypic variation in the majority of morphological (shoot and root), dry matter and cumulative water transpiration (CWT) traits in both treatments **(Fig. 1A-B)** and with substantial correlations among these traits **(Supplementary Figure S3A-B)**. The second PC, explaining >12% of the total variation, was mainly associated with root anatomical traits but a portion of the variation was also accounted for by root morphological traits such as specific root length (SRL) and two of its components: total root weight density (TRWD) and average root thickness (ART**; Fig. 1A-B)**. Moreover, these root anatomical and morphological traits were correlated with each other. For instance, SRL showed a negative correlation with

TRWD (on average r = -0.87), ART (r = -0.73), and all root anatomical traits (r = ca -0.30) in both treatments, except with late metaxylem number (LMXN) in control and stele diameter in proportion of root diameter (SD:RD) in both control and stress **(Supplementary Figure S3A-B)**. These results clearly indicate, that an increase in SRL could result in reducing the root thickness, stele diameter (SD) and late metaxylem diameter (LMXD). The first two components in control and water-deficit stress explained many of these complex relationships for most of the traits in this study (**Fig. 1**). In general, such relationships among traits might be due to pleiotropic or tightly linked genetic loci or gene, although that cannot be inferred directly from their positive and negative relationships.

High degree of trait variability in response to water-deficit stress underlies phenotypic plasticity

Phenotypic plasticity can have adaptive significance, while in some cases it can be an inevitable response under resource limitations (Nicotra et al., 2010). Significant treatment effects ($P < 0.001$) on all traits indicate expression of phenotypic plasticity under water-deficit stress. For most traits water-deficit stress resulted in lower values than observed for the control, with reductions ranging from 2 to 66%. Most of the root traits showed significant reductions. However, SRL, SD:RD, stem weight ratio (SWR), root length per unit leaf area (RLLA) and water use efficiency (WUE) were increased for plants grown under water-deficit stress than for plants under control conditions **(Supplementary Table S1)**. Roots were thinner under water-deficit stress than under control conditions as indicated by SRL (22% increase over control) and two of its components TRWD (20% decrease) and ART (11% decrease; **Fig. 2A-C**).

The rice root anatomy is adapted to semi-aquatic conditions with characteristic outer sclerenchymatous layer, large cortex diameter, small stele and xylem (Coudert et al., 2010;

Kadam et al., 2015). However, to what extent natural and human selection has shaped root anatomical plasticity in response to water-deficit stress remains to be elucidated. In this study, all root anatomical traits showed phenotypic plasticity to stress treatment (T: $P<0.001$) but lacked genotypic variability for plasticity (G×T: $P\geq0.05$) **(Supplementary Table S1 and Fig. 2D-I).** Cortex diameter (CD) showed a strong response (18% decrease; **Fig. 2E**) with low level of plasticity for stele diameter (SD; 4% decrease, **Fig. 2F**), LMXD (7% decrease; **Fig. 2H**) and LMXN (2 % decrease; **Fig. 2I**). These results are in agreement with a recent study involving three rice genotypes (Kadam et al., 2015). The reduced CD increases the relative area constituted by the stele (increased SD:RD; **Fig. 2G**) in roots, decreases radial distance, and improves radial hydraulic conductivity. The reduced CD could also significantly reduce the roots metabolic cost of soil exploration, thereby improving the water and nutrient acquisition in water-deficit and nutrient stress (Chimungu et al., 2014; Vejchasarn et al., 2016). However, reduced CD reduces the root thickness (**Fig. 2D**), thereby mechanical strength of the root, which is a key to penetrating soil hardening under water-deficit stress (Yoshida and Hasegawa, 1982).

Population structure and whole genome linkage disequilibrium

A balanced population structure and an optimal amount of linkage disequilibrium (LD) are important prerequisites for a successful GWAS, because the former corrects any confounding effect to avoid spurious associations whereas the LD is critical to infer the results (Mackay and Powell, 2007). The principal component analysis (PCA) with 46K SNPs (MAF≥0.05) revealed continuous distribution with no deep substructure in the 274 rice *indica* genotypes as indicated by the limited amount of genetic variation (only 19%) explained by the first four PCs (**Supplementary Figure S4A-B**). Likewise, the LD on average across chromosomes dropped to half of its initial value at ~55 to 65 kb and to the background levels ($r^2\leq0.1$) at

around ~600 kb to 1 Mb **(Supplementary Figure S5)**. The observed LD decay distance was significantly shorter than previously observed values in rice *indica* subgroups at ~100-125 kb (Zhao et al., 2011; Huang et al., 2010), indicating more historical recombination events in our studied population likely due to the diverse sampling of a wide range of landraces and breeding lines with a low degree of genetic relatedness. Hence, a higher resolution can be expected from the mapping efforts, although it would also depend on the local LD pattern near the significant peaks.

Single and multi-locus mapping identifying core regions of rice genome associated with stress adaptive traits

To elucidate the genetic architecture, we conducted GWAS on 33 traits (excluding two traits [RL3035 & RL35] that lacked genotypic variation) across treatments and of their plasticity with 46K, SNPs (MAF≥0.05) using a single-locus compressed mixed linear model (CMLM) and a multi-locus mixed model (MLMM; more details in Materials and Methods). **Table 2** provides a summary of GWAS for 33 traits from 5 categories. In total, we detected a nearly equal number of associations in control (104) and the water-deficit stress (106), although the significant loci varied across and within trait categories and treatments. Further, 22 out of 104 associations in control and 10 out of 106 in water-deficit conditions were linked with more than one trait, possibly due to tight linkages or pleiotropic effects of loci or genes. For plasticity of traits, we identified 76 associations (**Table 2 and Supplementary Tables S3-S5**), of which 9 were linked with more than one trait (**Supplementary Table S6**). Of the total loci, 22% in control, 33% in water-deficit stress and 27% for plasticity of the traits were detected commonly by both approaches with statistically improved power (lower *P* value) for most of the loci using the MLMM approach. In addition, MLMM identified additional novel loci in both treatments and for trait plasticity. In particular, MLMM identified significant loci

for some traits where CMLM failed to identify any loci, and the identified loci was mostly novel, although in a few cases already found to be associated with other traits in this study. For instance, we identified 4 and 3 loci for total root length (TRL) in control, and water-deficit stress conditions, respectively, only with MLMM, and one locus on chromosome 4 under stress was associated with root weight (RW) and root: shoot ratio (RS; **Supplementary Figures S6-S7**). Similarly, we identified 3 loci for CWT and 4 for WUE in water-deficit condition only through MLMM (**Supplementary Figure S8**). Thus, MLMM approach proved to be valuable in dissecting the genetic architecture of complex traits by identifying additional novel loci (Segura et al., 2012). The detailed GWAS results through CMLM and MLMM approach are given in **Supplementary Tables S3-S5**.

Quantitative variation of root morphology in two moisture regimes and their plasticity provides insights into complex genetic pattern

The genetic architecture of root traits is complex; determined by multiple small effect loci and studied extensively on mapping populations of rice representing the narrow genotypic base (Courtois et al., 2009). The genetic variations of root traits are relatively less characterized in diverse rice genotypes (Courtois et al., 2013; Phung et al., 2016; Biscarini et al., 2016) and can be a potential source for evolutionary beneficial alleles. Further, most of these studies have characterized the genetic variations in single isolated environments and not considered the two moisture regimes simultaneously, typically due to difficulty in the root phenotyping (space, time and cost). In this study, we carefully phenotyped the root traits in two moisture regimes and extracted the root morphology in various hierarchies by automated digital image analysis tool WinRHIZO (**Table 1;** materials and methods for root phenotyping). Through GWAS analysis, we detected 34 loci for 11 morphological, 1 for RW and 3 for RS in control and 52 loci for 12 morphological, 4 for RW

and 4 for RS ratio under water-deficit (**Table 2 and Supplementary Tables S3-S4**). The SRL is one of the important root morphological traits and often used as a proxy for root thickness. We observed 3 and 8 loci for SRL in control and stress conditions through CMLM and MLMM (**Fig. 3 and Supplementary Tables S3-S4**). The mean narrow-sense heritability (h^2) of root traits that showed significantly associated loci varied between 0.20 and 0.89 in control and between 0.32 and 0.78 in stress conditions (**Supplementary Table S2**). In addition, we identified 33 loci for 12 root morphological plasticity traits, one locus for rRW and four loci for rRS ratio, with mean h^2= 0.40 for traits that showed significant associations (**Table 2 and Supplementary Tables S2 and S5**). Above results clearly illustrate that variation in root plasticity is heritable and determined by the genetic factors.

Dividing a trait into multiple component traits unravels the underlying inherited complexity (Yin et al., 2002). We have detected an increased number of genetic loci for root length classified on root thickness than for TRL across treatments (**Supplementary Tables S3-S4 and S7**). For instance, we identified 4 loci in control and 3 loci in water-deficit stress for TRL. Mapping with root length traits of different root thickness classes resulted in identifying the additional 10 loci in control and 18 loci under water-deficit stress that were not detected by TRL *per se* (**Supplementary Table S7**). Similar result was observed for total weight (TW) and for its three component traits namely leaf weight (LW), stem weight (SW) and RW (**Supplementary Tables S3-S4**). These results clearly suggested that separating the complex trait into component traits improves the power to detect significant associations, perhaps by minimizing the variance between raw value and thereby increases the chance to detect variation in its component traits in agreement with previous study (Crowell et al., 2016). However, for plasticity, we identified only 5 loci for root length of different root thickness classes, of which 1 was common with rTRL and 4 were novel loci (**Supplementary**

Table S7). This lower number of loci for plasticity could also be due to the fact that plasticity is the trait ratio estimated from measurements across two treatments. Nevertheless, our ability to identify this distinct genetic loci when mapping the component traits might be capturing the key causal genetic regulator controlling the various aspects of root morphology. Moreover, there were no common loci detected either for TRL or its component traits across treatments, and this suggests that genetic control of root morphology is different across moisture regimes and strongly influenced by water-deficit. This could be further substantiated by all the novel loci identified for plasticity in the above traits, which might be a specific stress responsive genetic loci determining the plastic response.

Co-localization of root morphology loci explains underlying genetics and physiology

Many of the root traits and other traits result from complex combination of biological mechanisms controlling the expression in coordination as explained by their correlation. This correlation between traits could results from pleiotropic action of genetic loci on different traits or due to tight linkage between genetic loci. The root system supports the aboveground shoot growth through absorption of water and nutrients. In this study, one locus on chromosome 5 (7131196) was commonly associated with root morphology (RV, RL1015, RL1520), RW, CWT and TW in control condition (**Supplementary Table S6**). All these traits showed a positive (r=ca 0.65) correlation with CWT in control condition (**Supplementary Figure S3A**). In water-deficit stress, one locus on chromosome 1 (different SNP but falls within same LD block) was commonly associated with CWT (23207640) and SRL (23218344) and both these traits were negatively correlated (r=-0.34; **Supplementary Figure S3B**). Similarly, for plasticity, one locus on chromosome 7 (9463744) was commonly associated with rTRL, rSA (9463899; different SNP but falls within same LD block), rTLA and rCWT (**Supplementary Table S6**). To comprehend, these results clearly illustrate the

common genetic control of root morphology and water transpiration possibly to maintain the balanced hydraulic continuum between water uptake and transpiring organ. One locus on chromosome 9 (14829621) was commonly associated with root volume (RV), leaf weight ratio (LWR) and stem weight ratio (SWR), in water-deficit (**Fig. 4**). The minor allele at this locus had a positive effect on SWR and negative on RV and LWR (**Supplementary Table S4**); this further elucidates the negative correlation of SWR with RV and LWR (**Supplementary Figure S3B**). The same locus was associated with root length 0.5-1.0 mm diameter class (RL0510) and surface area (SA) in water-deficit stress (**Supplementary Table S6**). The ratio of root to shoot is more often used as an index of water-deficit stress tolerance and surrogate for root morphology. One locus on chromosome 4 (29111186) was commonly associated with TRL, RL005, RW and RS in water-deficit. The minor allele of this locus had a positive effect on all these traits (**Supplementary Table S4)**. Further, one of the significant loci was commonly detected in both the moisture regimes; associated with maximum root length (MRL) in control and SRL in water-deficit (**Supplementary Tables S3-S4)**. We also identified locus on chromosome 12 (25006932) commonly associated with plasticity of root morphology traits (rTRL, rRL005, rSA, rRV, rRTN and rRLD) and rTN (**Supplementary Table S6)**. These identified loci influencing multiple traits could be a potential marker for the marker assisted selection after validating in the elite genetic background.

Genetic basis of radial root anatomy

The functioning of roots is strongly depends on radial organization of root anatomy, which is regulated by the asymmetric cell division. The genetic control of radial root organization is less studied in rice, with largely unknown underlying genetic mechanisms. Understanding the genetic control of radial root anatomy is more challenging in rice because the complexity and size of the fibrous root system presented several phenotyping challenges. To date, only one

study in rice has identified the genomic regions for radial root anatomy (Uga et al., 2008). Through GWAS analyses, we identified 14 significant loci for 5 anatomical traits in control; 17 loci for 4 anatomical traits in water-deficit and 15 loci for the plasticity of 4 anatomical traits (**Table 2 and Supplementary Tables S3-S5**). Root diameter (RD; anatomical) of the adventitious root and ART (morphological) of the complete root system are positively correlated (control: r=0.22 and water-deficit: r=0.25) and a locus on chromosome 1 (1099857/1111294; different marker but fall within same LD block) was commonly associated in control condition (**Supplementary Table S6**). Both these traits are measures of root thickness, thus illustrate that measuring the RD at one position (near root-shoot junction) to some extent, was able to capture genetic variation of complete root system thickness. Three anatomical traits, namely RD, CD and SD:RD, were highly correlated with each other in control (**Supplementary Figure S3A**), and we found one common locus (21266079) associated with them on chromosome 7 (**Supplementary Table S6**). Stele tissue is the central part of the root enclosing the vascular cylinder (xylem and phloem), and one locus on chromosome 9 (13788883) and 5 (3057869) was commonly associated with SD and LMXD in stress (**Supplementary Table S6**). However, no locus was commonly detected across moisture regimes clearly suggest that genetic control of radial root anatomy is strongly influenced by stress. For anatomical plasticity, we observed two loci (11038867 and 11596350) on chromosome 1 common to rRD, rCD and rSD (**Supplementary Figure S9)** and plasticity of these traits was positively correlated with each other (**Supplementary Figure S3C)**. Hence, relative change in these traits in response to the water-deficit is partly under similar genetic control because they also have another independent associated genetic loci.

A priori candidate genes underlying the genetic loci of stress adaptive traits

A lower LD decay rate results in larger LD block and lower mapping resolution, which makes the GWAS not straightforward in identifying the causal genes. On average across genome LD decay rate was 55-65 kb in the studied population but then again, the association resolution varied with loci due to local LD pattern. Hence, we have calculated the LD pattern near to all the significant loci identified in this study (Materials and Method). In total, we have collected a list of 296, 284, and 233 *a priori* candidate gene within the expected LD block in control, water-deficit and for their plasticity, respectively. Of the total *a priori* candidate genes, 48 (control), 61 (water-deficit) and 38 (plasticity) genes were responsive to abiotic stress stimulus (**Table 2 and Supplementary Datasets S2-S4)**. Further, we have identified the list of 70 *a priori* genes close to significant loci for shoot morphological, physiological, dry matter traits in control (32 genes), water-deficit (21 genes) and for their plasticity (17 genes; **Supplementary Table S8**). For instance, one locus on chromosome 6 (13412649) for CWT and one on chromosome 9 (15426362) for WUE under stress was near to AQUAPORIN (AQP; 4 kb) and the WAX2 (66 kb) genes, respectively (**Supplementary Figure S8 and Supplementary Table S8**). The AQP gene is known to maintain root hydraulic conductivity, cell turgor, mesophyll conductance, water transpiration and thereby growth (Henry et al., 2012; Flexas et al., 2006), whereas WAX2 gene regulates epicuticular wax production, maintains cellular water status and improves the WUE (Chen et al., 2003), (Premachandra et al., 1994). Similarly, one locus on chromosome 2 (31650233) for tiller number (TN) in control was within ethylene-responsive transcription factor (ERFTF) gene and homologue of this gene was known to regulate rice tillering (Qi et al., 2011). Likewise, for all the root traits (root morphology and anatomy, RW and RS ratio), we have identified a list of 40, 57 and 41 *a priori* candidate genes in control, water-deficit and for their plasticity, respectively, with a role in root growth and development (**Supplementary Tables S9-S11**). Several genes were regulating root growth and development through phytohormone transport

and signalling (Auxin, ABA, GA, ethylene and brassinosteroid); cell division and differentiation; cellular redox homeostasis; molecular chaperone; water and nutrient transporter; cellular component organization and cell wall remodelling. For instance, one locus on chromosome 6 (366330) for RL0510 in control (**Supplementary Table S9**) was within the SCARECROW (SCR) gene that regulates radial root and shoot anatomy and root hair tip growth through cell division and differentiation (Gao et al., 2004). One locus on chromosome 1 (40526762) for RV in control was within the OsSAUR3 gene, an early auxin responsive gene that regulates root elongation (Markakis et al., 2013). The two homologues of this gene were close (OsSAUR25=11 kb and OsSAUR26=42 kb) to the locus on chromosome 6 (27819933) for MRL in control (**Supplementary Table S9)**. Likewise, in water-deficit conditions, a locus on chromosome 9 (14829621) was commonly associated with RV, RL0510, SA, LWR and SWR and was found within the GASA10 gene (**Fig. 5 and Supplementary Table S10)** . The GASA10 gene is known to participate in phytohormone crosstalk leading to redox homeostasis, and regulates root, stem and other organs growth (Nahirñak et al., 2012). For plasticity, one locus on chromosome 8 (26362631) for rSRL was near (30 kb) to an auxin efflux carrier component protein (AEC; **Supplementary Table S11**) and this gene is known to regulate auxin transport with mutant showing defective root development (Grieneisen et al., 2007).

Three interesting *a priori* candidate genes were recognized for radial root anatomy loci in this study. A locus on chromosome 11 (2838776) for LMXN in control was near (7 kb) to bHLH (basic helix-loop helix protein). The Arabidopsis orthologue LONESOME HIGHWAY having sequence similarity to bHLH and regulating the stele and xylem development (**Supplementary Table S9)**. Similarly, a locus on chromosome 11 (28871551) for LMXD in stress was within SCR (3 homologous copies in LD block), a gene that regulate radial

anatomy of root and shoot (**Supplementary Table S10)**; its homologue was associated with root morphology traits as discussed earlier. The LONESOME HIGHWAY gene regulates vascular tissue differentiation and number with involvement of auxin in Arabidopsis (Ohashi-Ito et al., 2013), while SCR is an auxin responsive gene regulating radial patterning in both root and shoot in Arabidopsis (Gao et al., 2004). Likewise, one of the locus on chromosome 9 (13788883) commonly associated with SD and LMXD in stress (**Supplementary Table S10**). This locus was near (24 kb) KANADI gene that regulates root development (Hawker and Bowman, 2004), and expressed during vascular tissue development (Zhao et al., 2005). In summary, many *a priori* candidate gene regulating the root morphology and radial root anatomy has been identified in this study.

Conclusions and future prospects

In the past mainly root morphological differences have been extensively (phenotypically and genetically) characterized with very little attention to radial root anatomy in rice. For the first time, we have characterized phenotypic variation for root morphological traits through powerful and intensive image-based systems and anatomical traits through microscopic dissection of root in a diverse set of rice *indica* genotypes across two moisture regimes. The single- and multi-locus GWAS analyses provided novel genetic insights that can help explain the observed genotypic variation of root morphological and anatomical traits across two moisture regimes. The phenotypic plasticity of the root morphology and anatomy was moderately heritable and had sufficient genetic control that resulted in identifying key core regions of rice genome. Thus, variation in root traits is a valuable resources that can result in identifying the potential novel genetic loci. Favourable alleles of these identified loci could after validation be directly used for marker-assisted selection. Many of these loci were either close to known genes or within genes themselves that play a role in root growth and

development. For example, several phytohormone genes influencing transport and signalling were found close to our identified loci, confirming well-known dominant role of these genes in root growth and development. The cloning and characterization of these genes can provide additional checkpoints in rice root growth and development. A further holistic approach of root system genetics is needed to be complemented with GWAS studies to understand the complexity of gene networks in controlling root growth and development. Future studies should also aim for more efficient high-throughput root phenotyping approaches both in field and control glasshouse conditions, to help advance root genetics.

Materials and Methods

Plant materials

For our GWAS study, we used a diverse collection of 274 genotypes covering traditional and improved *indica* rice sub-species, originating from major rice growing countries of tropical regions (**Supplementary Figure S1** and **Supplementary Dataset S1**). This panel was carefully assembled at the International Rice Research Institute (IRRI) for the Phenomics of Rice Adaptation and Yield potential (PRAY) project for use in GWAS studies (Al-Tamimi et al., 2016; Rebolledo et al., 2016; Kikuchi et al., 2017) in the context of the GRiSP Global Rice Phenotyping Network (http://ricephenonetwork.irri.org/).

Stress imposition and plant growth conditions

A pot experiment was carried out in natural greenhouse conditions at the International Rice Research Institute (IRRI), Philippines, for phenotyping root and shoot traits under two moisture regimes: (i) control, i.e., 100% field capacity (FC) that is defined as the maximum soil moisture content after draining excess water, and (ii) water-deficit stress at 55 to 60% FC. The experiment was laid out in a randomized complete block design and replicated over

three different time periods, due to space and labour constraints, during 2012-2013 (**Supplementary Figure S10A**). Before sowing, rice seeds were exposed to 50 $^{\circ}$C for 3 days to break dormancy and pre-germinated seeds were sown in white-coloured painted pots (55 cm long and 15 cm diameter) to minimize confounding effects of increasing temperature of pot surface and soil (Poorter et al., 2012). The pots were lined with polythene bags on the inside, filled with 11 kg of clay loam soil and care was taken to avoid over-compaction of the soil. Each pot had two holes at the bottom for imposing controlled stress. Water-deficit stress was imposed 15 days after seedling emergence (after ensuring healthy seedling establishment) and until then all pots were maintained at 100% FC (**Supplementary Figure S10B**). A standardized gravimetric approach of daily pot weighing (Kadam et al., 2015) was followed on 1649 (5 pots were empty to measure evaporation) pots to gradually attain 55-60% FC and thereafter maintained at the same level until the end of the experiment (**Supplementary Figure S10C**). Once the target stress level was reached, daily water loss due to evapo-transpiration was replenished by adding back an exact amount of water to bring back the moisture content to the desired target in each pot. Soil surface was covered with a circular polythene sheet to protect direct evaporative loss of water and a slit across the radius of the polythene prevented heat build-up on the soil surface. Additionally, a set of soil filled pots without a plant was also maintained to correct for evaporative loss of water from the opening created by slit in the circular shaped polythene sheet. Daily pot weights recorded for 30 consecutive days of stress period were used to calculate the daily evapo-transpiration. After correcting for evaporative loss obtained from empty pots, actual transpiration was calculated. Finally, daily actual transpiration was summed for the 30-day period to calculate cumulative water transpired. Whole plant water use efficiency (g kg^{-1}) was calculated as a ratio of total weight (root and shoot) to cumulative water transpired. Air temperature and humidity were constantly measured at 10-minute intervals by sensors installed in the

greenhouse. The average daily temperature (day and night) and air humidity were recorded (**Supplementary Figure S10D**).

Shoot and root harvesting

After 30 days of water-deficit stress exposure, plants were harvested at 45 days after sowing and tiller numbers were counted and total leaf area was estimated by a leaf area meter (Li-3000, LI-COR, Lincoln, NE, USA). Leaves and stems were separately oven-dried at 70 °C for 72 h to compute the specific leaf area and shoot weight. The entire column of soil along with the roots was placed on a large 1 mm sieve and meticulously washed using a gentle stream of water to minimize the loss of small roots and root hairs.

A strong plasticity in wheat root anatomy primarily near root-shoot junction (RSJ) and root tips under water-deficit stress has been confirmed following a similar approach (Kadam et al., 2015). Hence, three replicate root sections were collected near the RSJ (~7-10 cm) from control (274×3=822) and water-deficit stressed (274×3=822) samples (1644 samples). Collected samples were stored in 40% (v/v) alcohol for assessing root anatomy. The remaining whole-plant root samples were placed in 20% (v/v) alcohol and stored at 4 °C for root scanning and image analysis.

Root image acquisition and processing in WinRHIZO

Root samples stored in 20% (v/v) alcohol were cut to smaller segments to fit the scanner tray and aligned vertically on scanning plates to avoid overlapping (**Supplementary Figure S11**). An 8-bit greyscale image was acquired by scanning with an Epson Perfection 7000 scanner at a resolution of 600 dots per inch next to a ruler. After capturing the images, root samples were oven dried at 70 °C for 72 h to record the root weight. In total, we captured ~45, 000 images from 274 genotypes across treatments and replications. The root morphological

attributes such as total root length, average root thickness, root length classified based on root thickness, root volume, root surface area were computed by analysing images with WinRHIZO Reg 2012b (**Supplementary Figure S11**) software (http://regent.qc.ca/assets/winrhizo_about.html). To avoid underestimation of fine root lengths during image processing, the threshold which separates the roots and background was adjusted to automatic mode (Bouma et al., 2000).

Root anatomical study

To study the root anatomical parameters near root-shoot junction (~7-10 cm; **Supplementary Figure S12**), samples stored in 40% alcohol were hand sectioned with a razor blade under the dissection microscope. Images of root sections were acquired with Zeiss Axioplan 2 compound microscope (Zeiss, Germany) with 50× and 100× magnification. At least 3-5 root images per replicate were considered for measuring anatomical parameters such as root cross-section diameter, stele diameter and late meta xylem diameter, with image J software (Schneider et al., 2012).

Derived shoot, root and water uptake parameters

Average specific leaf area was calculated as the ratio of total leaf area to leaf dry weight. Ratios of leaf weight, stem weight and root weight to total weight were also calculated. Root length density was calculated as the ratio of total root length to the soil volume in pot, and Total root weight density was calculated as the ratio of root weight to root length density. Specific root length was calculated as the ratio of total root length to root weight. Root length per unit leaf area was calculated as the ratio of total root length to leaf area.

Calculation of phenotypic plasticity

The phenotypic plasticity of all traits was calculated as a relative change in water-deficit stress compared to control conditions, using the formula (Sandhu et al., 2016).

$$Phenotypic\ plasticity = \frac{stress - control}{control}$$

To distinguish trait plasticity from the trait *per se*, all acronyms for plasticity starts with small letter "r" (**Table 1**).

Statistical data analysis

The observed variation in a phenotypic trait can be partitioned to a source of variation in genotype (G), treatment (T) and their interaction (G×T). The analysis of variance was performed using mixed linear model (MLM) for each phenotypic trait in Genstat release 17.1, as defined by

$$y_{ijk} = \mu + G_i + T_j + (G\times T)_{ij} + r_{k(j)} + e_{ijk}$$

where y_{ijk} is the measured trait, μ is the overall mean, G_i is the effect of i^{th} genotype, T_j is the effect of j^{th} treatment, $(G\times T)_{ij}$ is the interaction between i^{th} genotype and j^{th} treatment, $r_{k(j)}$ is the effect of replication k within the j^{th} treatment and e_{ijk} is the random error. Genotypic and treatment effects were considered as fixed effect with their interaction (G×T term) in the model and replications were treated as random effect. The best linear unbiased estimator (BLUE) value of each phenotypic trait was computed separately across treatments by MLM. The BLUE value of traits was later used for histograms, boxplots, principal component analysis (PCA) and Pearson's correlation analysis. The PCA analysis was performed in XLSTAT and correlation heat maps were compiled using the R package "corrplot" in R studio. The *P* values of correlation coefficient were calculated by two-sided t-test using the cor.mtest function in R and only significant ($P<0.05$) correlation was plotted on the heat maps.

SNPs genotyping data

The studied panel is a large subset of 329 *indica* genotypes that were genotyped using the genotype by sequencing (GBS) protocol (Elshire et al., 2011) at Cornell University, USA. The reads were demultiplexed and aligned to the rice reference genome (Os-Nipponbare-Reference-IRGSP-1.0) (Kawahara et al., 2013), and variants were identified using the NGSEP pipeline (Duitama et al., 2014). Missing data was imputed with the implementation of the Fast Phase Hidden Markov Model (Scheet and Stephens, 2006).

Two different datasets with different missing SNPs imputation from GBS sequencing data were recently used in GWAS analysis for this panel, i.e., the 90K SNPs dataset with 22.8% missing imputation by Rebolledo et al., 2016 and 45K SNPs dataset with 8.75% missing imputation by Kikuchi et al., 2017. In addition, this panel was also genotyped with a 700K SNPs dataset and recently used in a GWAS ((Al-Tamimi et al., 2016)). However, only 240 out of 274 genotypes used in our study were overlapped with quality SNPs. Thus, we have used the 45K SNPs dataset with 8.75% missing imputation that was more precise than the 90K SNPs dataset with higher percentage of missing imputation. The original dataset contains 46,999 SNPs with minor allele frequency (MAF) ≥ 0.05 and 8.75% missing data for 329 genotypes. We selected the SNP data for 274 genotypes phenotyped in our study with another round of MAF (≥ 0.05) filtering resulting in the final dataset containing 45,608 SNPs. The ≥ 0.05 of MAF was used to reduce the spurious association caused by rare variants.

Single-locus genome-wide association analysis

The single-locus GWAS analysis was performed on 45,608 SNPs and phenotypic traits by compressed mixed linear model (CMLM) (Zhang et al., 2010) in the Genomic Association and Prediction Integrated Tool (GAPIT) (Lipka et al., 2012). We incorporated population

structure (Q matrix as a PCA component) matrix (**Supplementary Figure S4A-B**) and family kinships (K) matrix (**Supplementary Figure S13**) calculated with 45,608 SNPs:

$$Y = X\alpha + P\beta + K\mu + e$$

where Y and X represent the vector of phenotype (BLUE) and genotype (SNP) respectively, P is the PCA matrix and K is the relative kinship matrix. Xα and Pβ is the fixed effects, and Kμ is the random effect and e represent the random error. The P and K terms were introduced to correct for false positive association. Although correction for the population structure substantially reduces false positives, it sometimes eliminates the true positive association due to overcorrection (Zhao et al., 2011). Therefore, the optimal number of PCs were determined for each trait before incorporating into CMLM, based on forward model selection using the Bayesian information criterion (BIC). Such statistical methods help to control both false positive and false negative associations effectively although they cannot eliminate both completely. Most of the root traits are complex polygenic in nature and we expected that the effect of the individual underlying loci would be small. Therefore, we chose a suggestive threshold of the probability *P* value ≤1.00E-04 to detect significant associations, as followed recently for the same population (Rebolledo et al., 2016) and in many other rice GWAS studies (Zhao et al., 2011; Norton et al., 2014; Dimkpa et al., 2016). The similar threshold was also used in another GWAS study for rice root traits (Courtois et al., 2013).

Broad-sense and narrow-sense heritability

Phenotypic variance can be decomposed into variance caused by genetic and environmental factors. The broad sense heritability (H^2) is the proportion of phenotypic variance that is due to genetic variance. Genetic variance can be a result of additive, dominance or epistatic effects. . The broad-sense heritability (H^2) of traits was calculated across each treatment as

$$H^2 = \frac{\sigma_G^2}{\sigma_G^2 + \frac{\sigma_E^2}{r}}$$

where σ^2_G and σ^2_E are the genotypic and residual variance respectively and r is the number of replications. The restricted maximum likelihood estimate was used to calculate the variance components in Genstat 17.1. The narrow-sense heritability is the proportion of phenotypic variance that is due to additive genetic variance. The marker-based narrow sense heritability (h^2) was obtained from above mentioned CMLM equation and was calculated using following equation in GAPIT

$$h^2 = \frac{\sigma_a^2}{\sigma_a^2 + \sigma_e^2}$$

where σ^2_a is the additive genetic variance and σ^2_e is the residual variance.

Multi-locus genome wide association analysis

In addition to correcting the confounding effect of population structure (first three PCA components) and family kinships (K) matrix, multi-locus linear mixed model (MLMM) corrects the confounding effect of background loci may be present due to LD in the genome (Segura et al., 2012). This was done by explicitly using loci as cofactors in the statistical model, similar to standard composite interval mapping of bi-parental analysis (Jansen and Stam, 1994). The multi-locus GWAS was implemented in the modified version of MLMM in R studio (R script for mlmm.cof.r available at https://cynin.gmi.oeaw.ac.at/home/resources/mlmm). First, we ran the complete model as recommended with stepwise forward inclusion of the strongest significant markers as a cofactor until the heritability reached close to zero, and after that backward elimination of the least significant markers from the model was carried out with estimating the variance components and *P* values at each step (Segura et al., 2012). In the second step we checked the optimal model selection using the available criteria in MLMM: (i) extended Bayesian

information and (ii) the multiple Bonferroni. However, both these criteria were too conservative to identify loci for most of the traits in our study and identified significant loci for very few traits (LMXN, RS, SW and SWR) only in water-deficit stress condition. Therefore, we checked the *P* value of markers at first step (similar to single locus GWAS analysis with no cofactor in the model) before including them as a cofactor and continued the model with inclusion of markers as a cofactor on an arbitrary cut-off significance threshold *P* value ≤1.00E-04 as used in the single-locus GWAS analysis. Model was stopped when no significant loci appeared above the cut-off threshold *P* value and all significant cofactors with this approach were considered as a significant genetic loci.

Linkage disequilibrium (LD) analysis

The pair wise LD was calculated for the whole panel using the correlation coefficient (r^2) between pairs of SNPs on each chromosome by setting the sliding window at 100 in TASSEL 5.0 (Bradbury et al., 2007). A total of 45,608 SNPs with MAF (≥ 0.05) were considered for LD analysis. To investigate the LD decay rate, the r^2 values of the chromosome and average across the chromosome representing the whole genome LD pattern were plotted against the physical distance (kb) among the markers. The LD decay rate was measured as the physical distance (kb) at which r^2 value drops to half of its initial value.

***A priori* candidate gene selections**

The variation in recombination rates (an essential determinant of LD structure) could have broken the chromosome into a series of discrete haplotype LD block that determining the actual resolution of association mapping. The upper limit of LD decay rate is ~500 kb in rice (Mather et al., 2007). Therefore, we have selected ~0.5 to 0.6 Mb (total ~1.1 Mb) region on each side of the significant SNPs identified through GWAS analysis, to investigate the local

LD pattern near to the significant SNPs (Huang et al., 2010). The Haploview 4.2 program was used to calculate LD structure near the significant SNPs (Barrett et al., 2005) and visualize the discrete haplotype block in ~ 1.1 Mb region. The LD haplotype block harbouring the significant SNP or more than one significant SNPs was identified and considered as a unique significant locus. The known genes (genes with known annotation) located within LD blocks were collected. The closest Arabidopsis orthologue genes were obtained from the MSU7 Rice genome database (http://rice.plantbiology.msu.edu/cgi-bin/gbrowse/rice/). All the genes described as a transposon and retro transposon were not selected and genes described as an expressed protein (EP) was considered only when there is relevant information available from Arabidopsis orthologue.

URLs.

WinRHIZO root image analysis, http://regent.qc.ca/assets/winrhizo_about.html/;

R version of MLMM, https://cynin.gmi.oeaw.ac.at/home/resources/mlmm/;

Michigan State University (MSU) Genome Browser, http://rice.plantbiology.msu.edu/cgi-bin/gbrowse/rice/.

ACKNOWLEDGEMENTS

This work was supported by an anonymous private donor who provided the financial support, via Wageningen University Fund, to the first author's PhD fellowship and field work at IRRI. We also thank The Federal Ministry for Economic Cooperation and Development, Germany, and the USAID-Bill & Melinda Gates Foundation for their financial support. Dr. G. van der Linden and Dr. P.S. Bindraban are acknowledged for their valuable advice.

COMPETING FINANCIAL INTERESTS

The authors declare no competing financial interests.

Figure 1. Principal component analysis of the 35 traits with first two components showing variation in control **(Panel A),** and water-deficit stress **(Panel B)** conditions. The traits marked by dashed ellipses contributing more to the variation explained by the PC1 and marked by solid circle/ellipses to PC2. Trait labels coloured differently according to category (uppercase letter in each panel) in Table 1; acronyms are given in the Table 1 as well.

Figure 2. Overlying histograms with normal distribution curves (control: green line, dark grey bars; water-deficit stress: red line, light grey bars; intermediate grey: overlap for the treatment with the lower frequency value) showing the phenotypic distribution of root morphological **(Panel A-C)** and anatomical **(Panel D-I)** traits. The vertical lines in the histograms show population mean values in control (green) and water-deficit stress (red) conditions and values in parentheses represent the significant percentage change (+: increase or –: decrease) in water-deficit stress conditions over the control. Levels of significance for Genotype (G), Treatment (T) and their interaction (G×T) effects from ANOVA are given in the histograms (***, $P<0.001$; ns, not significant).

Figure 3. GWAS results through the compressed mixed linear model (CMLM) and the multi-locus mixed model (MLMM) approaches for specific root length (SRL) in control (the two upper panels) and water-deficit conditions (the two middle panels) and the trait plasticity calculated as the relative value of the water-deficit stress conditions over the control (the two bottom panels). Significant SNPs (coloured red in the Manhattan plots) are distinguished by threshold *P* value lines (solid black= [$-\text{Log}_{10}$ P >4] and dotted black= Bonferroni-corrected threshold). Significant SNPs in MLMM Manhattan plots are numbered in the order that they were included in the model as a cofactor. *A priori* candidate genes (**Supplementary Tables S9-S11**) are indicated near to peak SNP/SNPs in the Manhattan plot. **AEC:** auxin efflux carrier; **ABC:** ATP-binding cassette transporters; **SULT:** Sulfate transporter; **PPR:** Pentatricopeptide; **IPT:** Inorganic phosphate transporter; **BTB1:** Brick-Brack, Tramtrack, Broad Complex BTB, **EP:** Expressed protein; **Gα:** G-protein alpha subunit; **SAUR:** Small auxin UP-RNA; **PG:** Polygalacturonase; **NAM:** No apical meristem.

Figure 4. GWAS results through compressed mixed linear model (CMLM) and multi-locus mixed model (MLMM) approaches (Manhattan and Quantile-Quantile plots) for root volume (RV), leaf weight ratio (LWR) and stem weight ratio (SWR) in water-deficit stress. Significant SNPs (coloured red in the Manhattan plots) are distinguished by threshold *P* value lines (solid black= [$-\text{Log}_{10}$ P >4] and dotted black= Bonferroni-corrected significance threshold) and coloured red in the Manhattan plots (**Panel A**). Significant SNPs on MLMM Manhattan plots are numbered in the order that they were included in the model as a cofactor. Identified LD blocks based on pairwise r^2 values between SNPs on chromosome 9 (**Panel B**) with *a priori* candidate gene in the underneath table (for more details see **Supplementary Tables S8 and S10**). The colour intensity of the box corresponds with r^2 value (multiplied by 100) according to the legend. Significant SNP ("**14829621"**) marked in yellow rectangle was commonly associated with RV, LWR and SWR **(Panel B)**. **PPR:** Pentatricopeptide, **CLV1:** CLAVATA1; **Gβ:** G-protein beta subunit; **OXR:** Oxidoreductase; **POX:** Peroxidase; **KT:** Potassium transporter

SUPPLEMENTAL DATA

Supplementary Figure S1. Geographical origin of 273 rice *indica* genotypes grown in tropical regions of the world and one genotype without available information.

Supplementary Figure S2. The Principal Component Analysis scree plot of 35 phenotypic traits across 274 genotypes depicting the variation explained by each component (PC) in control **(Panel A)** or water-deficit stress **(Panel B)** conditions.

Supplementary Figure S3. Pearson correlation coefficients between 35 phenotypic traits in control **(Panel A),** water-deficit stress (**Panel B**) conditions and for the plasticity of traits **(Panel C)**.

Supplementary Figure S4. The Principal Component analysis constructed on 46K SNPs (MAF $\geq$ 0.05) across 274 genotypes with first two components depicting the population structure **(Panel A).**

Supplementary Figure S5. Individual chromosome and average genome wide linkage disequilibrium decay as a measure of r^2 between the pairs of SNPs over the physical distance on the genome.

Supplementary Figure S6. The GWAS result through the compressed mixed linear model (CMLM) and the multi-locus mixed model (MLMM) approaches for total root length (TRL) in control and water-deficit stress conditions and for its plasticity as a relative measure.

Supplementary Figure S7. The GWAS result through the compressed mixed linear model (CMLM) and multi-locus mixed model (MLMM) approaches for root weight (RW) and root.

Supplementary Figure S8. The GWAS result through the compressed mixed linear model (CMLM) and multi-locus mixed model (MLMM) approaches for cumulative water transpiration (CWT) and water use efficiency (WUE) in water-deficit stress condition.

Supplementary Figure S9. The GWAS result through the compressed mixed linear model (CMLM) and multi-locus mixed model (MLMM) approaches for plasticity as the relative value of the water-deficit stress over the control conditions for root diameter (rRD), cortex diameter (rCD) and stele diameter (rSD).

Supplementary Figure S10. The experimental setup for phenotyping a diverse set of 274 rice genotypes under greenhouse experiment for phenotypic traits **(Panel A).**

Supplementary Figure S11: Illustrative root image analysis with WinRHIZO programme displaying the measurement of root morphological traits.

Supplementary Figure S12: The root anatomical trait variation of two rice genotypes near root-shoot junction in control conditions.

Supplementary Figure S13. The heat map of kinship matrix defining genetic relatedness across 274 genotypes with red and yellow colour indicates the highest and lowest correlation

Supplementary Table S1. Descriptive statistics and the significance of *P* (Wald test summary) value based on a linear mixed model for genotype (G), treatment (T) and their interactions (G×T). For more details on trait acronyms and units see the Table 1.

Supplementary Table S2. Broad-sense (H^2) heritability for 35 phenotypic traits classified in 5 (A-E) categories in control (C) and water-deficit stress (WD) conditions.

Supplementary Table S3. Summary of identified genome-wide significant association loci for phenotypic traits in control condition using compressed mixed linear model (CMLM) and multi-locus mixed model (MLMM) approaches.

Supplementary Table S4. Summary of identified genome-wide significant association loci for phenotypic traits in water-deficit condition using compressed mixed linear model (CMLM) and multi-locus mixed model (MLMM) approaches.

Supplementary Table S5. Summary of identified genome-wide significant association loci for plasticity of phenotypic traits using compressed mixed linear model (CMLM) and multi-locus mixed model (MLMM) approaches.

Supplementary Table S6: Genetic loci associated with more than one phenotypic traits in control (22 loci), water-deficit stress (10 loci) and for phenotypic plasticity (9 loci).
Supplementary Table S7. Genetic loci for total root length (TRL) and root length of different root thickness classes (as a component traits of TRL) in control (C), water-deficit (WD), and for their phenotypic plasticity (PP).
Supplementary Table S8: The *a priori* candidate genes underlying different loci/locus of shoot morphological, physiological, dry matter traits in control (C; 32 genes), water-deficit stress conditions (WD; 21 genes) and for its phenotypic plasticity (PP;17 genes) as a relative measure.
Supplementary Table S9: The predicted *a priori* candidate genes (total 40 unique *a priori* genes excluding loci associated with more than one trait) underlying different loci/locus of root traits in control (C) condition and demonstrating to play a role in root growth and development.
Supplementary Table S10: The predicted *a priori* candidate genes (total 57 unique *a priori* genes excluding loci associated with more than one trait) underlying different loci/locus of root traits in water-deficit stress (WD) conditions and demonstrating to have a role in root growth and development.
Supplementary Table S11: The *a priori* candidate genes (41 *a priori* genes) underlying different loci/locus for plasticity of root traits as the relative value of the water-deficit stress treatment over the control treatment and demonstrating to have a role in root growth and development.
Supplementary Dataset S1
Supplementary Dataset S2
Supplementary Dataset S3
Supplementary Dataset S4

Supplementary Figure S1. Geographical origin of 273 rice *indica* genotypes grown in tropical regions of the world and one genotype without available information. The size of the symbol on the world map corresponds to the number of genotypes .

Supplementary Figure S2. The Principal Component Analysis scree plot of 35 phenotypic traits across 274 genotypes depicting the variation explained by each component (PC) in control **(Panel A)** or water-deficit stress **(Panel B)** conditions. The PC1 to PC8 with eigenvalues greater than 1.0 (green value above bars) were considered significant and cumulatively explained >80 % total variation.

Supplementary Figure S3. Pearson correlation coefficients between 35 phenotypic traits in control **(Panel A),** water-deficit stress (**Panel B**) conditions and for the plasticity of traits **(Panel C)**. The blue and red colours indicate positive and negative correlations, respectively. Colour intensity and size of the circle are proportional to the strength of correlation coefficients between the pair of traits. Uppercase letters on the left panels of the figure correspond with trait classifications as in Table 1; for trait acronyms and units see the Table 1.

Supplementary Figure S4. The Principal Component analysis constructed on 46K SNPs (MAF ≥ 0.05) across 274 genotypes with first two components depicting the population

structure **(Panel A).** The scree plot shows the variation explained by each principal component in proportion **(Panel B).**

Supplementary Figure S5. Individual chromosome and average genome wide linkage disequilibrium decay as a measure of r^2 between the pairs of SNPs over the physical distance on the genome. The r^2 was calculated using the 100 bp sliding window in the TASSEL 5 programme.

Supplementary Figure S6. The GWAS result through the compressed mixed linear model (CMLM) and the multi-locus mixed model (MLMM) approaches for total root length (TRL) in control and water-deficit stress conditions and for its plasticity as a relative measure. Significant SNPs (coloured red in the Manhattan plots) are distinguished by a threshold *P* value lines (solid black=[$-\text{Log}_{10}$ *P* >4] and dotted black=Bonferroni-corrected significance threshold). Significant SNP on MLMM Manhattan plots are numbered in the order that they were included in the model as a cofactor (cof in Quantile-Quantile plot is for cofactor). *A priori* candidate genes (see the **Supplementary Tables S9-S11**) are indicated near to peak SNP in the Manhattan plot.

Supplementary Figure S7. The GWAS result through the compressed mixed linear model (CMLM) and multi-locus mixed model (MLMM) approaches for root weight (RW) and root: shoot ratio (RS) in water-deficit stress condition. Significant SNPs (coloured red in the Manhattan plots) are distinguished by a threshold *P* value lines (solid black=[$-\text{Log}_{10}$ *P* >4] and dotted black=Bonferroni-corrected significance threshold). Significant SNP on MLMM Manhattan plots are numbered in the order that they were included in the model as a cofactor (cof in Quantile-Quantile plot is for cofactor). *A Priori* candidate genes (see the **Supplementary Table S10**) are indicated near to peak SNP/SNPs in the Manhattan plot.

Supplementary Figure S8. The GWAS result through the compressed mixed linear model (CMLM) and multi-locus mixed model (MLMM) approaches for cumulative water transpiration (CWT) and water use efficiency (WUE) in water-deficit stress condition. Significant SNPs (coloured red in the Manhattan plots) are distinguished by a threshold *P* value lines (solid black=[$-\text{Log}_{10}$ *P* >4] and dotted black=Bonferroni-corrected significance). Significant SNP on MLMM Manhattan plots are numbered in the order that they were included in the model as a cofactor (cof in Quantile-Quantile plot is for cofactor). *A priori* candidate genes (see the **Supplementary Table S8**) are indicated near to peak SNP/SNPs in the Manhattan plot.

Supplementary Figure S9. The GWAS result through the compressed mixed linear model (CMLM) and multi-locus mixed model (MLMM) approaches for plasticity as the relative value of the water-deficit stress over the control conditions for root diameter (rRD), cortex diameter (rCD) and stele diameter (rSD). Significant SNPs (coloured red in the Manhattan plots) are distinguished by a threshold *P* value lines (solid black=[$-\text{Log}_{10}$ *P* >4] and dotted black=Bonferroni-corrected significance). Significant SNP on MLMM Manhattan plots are numbered in the order that they were included in the model as a cofactor (cof in Quantile-Quantile plot is for cofactor). *A priori* candidate genes (see the **Supplementary Table S11**) are indicated near to peak SNP in the Manhattan plot.

Supplementary Figure S10. The experimental setup for phenotyping a diverse set of 274 rice genotypes under greenhouse experiment for phenotypic traits **(Panel A).** The procedure

followed to set up the experiment and to maintain two moisture regimes **(Panel B).** The rate of water depletion from the soil was calculated for each genotype based on the pot weighing data and expressed in moisture content in % field capacity **(Panel C).** Average daily day and night temperature and relative humidity during the growing period across the three independent replications **(Panel D).** Bars in panels C and D are the standard error of mean.

Supplementary Figure S11: Illustrative root image analysis with WinRHIZO programme displaying the measurement of root morphological traits. The dissimilar colour for roots indicates the different root length diameter class. For instance, red colour indicates the root length in 0.0-0.5 mm dimeter class. The left side on images shows the measurement of root morphological traits such as **Len**= root length (cm); **SA**=surface area (cm^2); **Vol**= root volume (cm^3); **AvgD**=average diameter (**mm**) that we renamed to average thickness to avoid misperception with measured root anatomical diameter.

Supplementary Figure S12: The root anatomical trait variation of two rice genotypes near root-shoot junction in control conditions. **RD**: root diameter, **CD**: cortex diameter, **SD**: stele diameter, **LMXD**: late metaxylem diameter and **LMXN**: late metaxylem number. Scale bar on root morphology image is 50 cm and on root anatomy is 100 µm. The table on image displays mean root anatomical variation measured across three replications.

Supplementary Figure S13. The heat map of kinship matrix defining genetic relatedness across 274 genotypes with red and yellow colour indicates the highest and lowest correlation between pairs of the genotypes respectively. A hierarchical clustering between genotypes is based on kinship values.

Supplementary Table S1. Descriptive statistics and the significance of *P* (Wald test summary) value based on a linear mixed model for genotype (G), treatment (T) and their interactions (G×T). For more details on trait acronyms and units see the Table 1.

Supplementary Table S2. Broad-sense (H^2) heritability for 35 phenotypic traits classified in 5 (A-E) categories in control (C) and water-deficit stress (WD) conditions. The narrow-sense (h^2) heritability of 35 phenotypic traits in C, and WD conditions and for their phenotypic plasticity (PP). The details on trait acronyms and units are given in the Table 1.

Supplementary Table S3. Summary of identified genome-wide significant association loci for phenotypic traits in control condition using compressed mixed linear model (CMLM) and multi-locus mixed model (MLMM) approaches. The loci commonly detected through both the approaches were marked by an asterisk sign (*) and those detected through only MLMM were marked by a hashtag sign (#). All the other unmarked loci were detected only through the CMLM approach. Trait acronyms are given in the Table 1.

Supplementary Table S4. Summary of identified genome-wide significant association loci for phenotypic traits in water-deficit condition using compressed mixed linear model (CMLM) and multi-locus mixed model (MLMM) approaches. The loci commonly detected through both the approaches were marked by an asterisk sign (*) and those detected through only MLMM were marked by a hashtag sign (#). All the other unmarked loci were detected only through the CMLM approach. Trait acronyms are given in the Table 1.

Supplementary Table S5. Summary of identified genome-wide significant association loci for plasticity of phenotypic traits using compressed mixed linear model (CMLM) and multi-

locus mixed model (MLMM) approaches. The loci commonly detected through both the approaches were marked by asterisk sign (*) and those detected through only MLMM were marked by a hashtag sign (#). All the other unmarked loci were detected only through the CMLM approach. Trait acronyms are given in the Table 1.

Supplementary Table S6: Genetic loci associated with more than one phenotypic traits in control (22 loci), water-deficit stress (10 loci) and for phenotypic plasticity (9 loci).

Supplementary Table S7. Genetic loci for total root length (TRL) and root length of different root thickness classes (as a component traits of TRL) in control (C), water-deficit (WD), and for their phenotypic plasticity (PP). Genetic loci (L) for TRL and its component traits are numbered from L1 to L14 (C), L15 to L35 (WD) and L36-L44 (PP). In the table, numbers are significant SNPs position and superscript numbers in brackets are chromosome number. SNPs number with number in bracket are assigned to unique loci and common loci are indicated only by genetic loci mentioned in brackets. †=novel loci identified for TRL component traits only.

Supplementary Table S8: The *a priori* candidate genes underlying different loci/locus of shoot morphological, physiological, dry matter traits in control (C; 32 genes), water-deficit stress conditions (WD; 21 genes) and for its phenotypic plasticity (PP;17 genes) as a relative measure. *A priori* candidate gene annotations in bold were responsive to abiotic stress stimulus (Gene Ontology:0009628) according to Rice genome browser database. Trait acronyms are given in the Table 1. †=Distance of gene from peak SNP.

Supplementary Table S9: The predicted *a priori* candidate genes (total 40 unique *a priori* genes excluding loci associated with more than one trait) underlying different loci/locus of root traits in control (C) condition and demonstrating to play a role in root growth and development. *A priori* candidate gene annotations in bold are responsive to abiotic stress stimulus (Gene Ontology:0009628) according to Rice genome browser database. Trait acronyms are given in the Table 1. †=Distance of gene from peak SNP.

Supplementary Table S10: The predicted *a priori* candidate genes (total 57 unique *a priori* genes excluding loci associated with more than one trait) underlying different loci/locus of root traits in water-deficit stress (WD) conditions and demonstrating to have a role in root growth and development. Candidate *a priori* gene annotations in bold are responsive to abiotic stress stimulus (Gene Ontology:0009628) according to Rice genome browser database. Trait acronyms are given in the Table 1. †=Distance of gene from peak SNP.

Supplementary Table S11: The *a priori* candidate genes (41 *a priori* genes) underlying different loci/locus for plasticity of root traits as the relative value of the water-deficit stress treatment over the control treatment and demonstrating to have a role in root growth and development. Candidate *a priori* gene annotations in bold are responsive to abiotic stress stimulus (Gene Ontology:0009628) according to the rice genome browser database. Trait acronyms are given in the Table 1. †=Distance of gene from peak SNP.

Supplementary Dataset S1
Supplementary Dataset S2
Supplementary Dataset S3
Supplementary Dataset S4

LITERATURE CITED

Al-Tamimi N, Brien C, Oakey H, Berger B, Saade S, Ho YS, Schmöckel SM, Tester M, Negrão S (2016) Salinity tolerance loci revealed in rice using high-throughput non-invasive phenotyping. Nat Commun **7:** 13342

Barrett JC, Fry B, Maller J, Daly MJ (2005) Haploview: analysis and visualization of LD and haplotype maps. Bioinformatics **21:** 263-265

Bernier J, Serraj R, Kumar A, Venuprasad R, Impa S, R.P VG, Oane R, Spaner D, Atlin G (2009) The large-effect drought-resistance QTL qtl12.1 increases water uptake in upland rice. Field Crop Res **110:** 139-146

Biscarini F, Cozzi P, Casella L, Riccardi P, Vattari A, Orasen G, Perrini R, Tacconi G, Tondelli A, Biselli C, Cattivelli L, Spindel J, McCouch S, Abbruscato P, Valé G, Piffanelli P, Greco R (2016) Genome-wide association study for traits related to plant and grain morphology, and root architecture in temperate rice accessions. PLoS ONE **11:** e0155425

Bouma TJ, Nielsen KL, Koutstaal B (2000) Sample preparation and scanning protocol for computerised analysis of root length and diameter. Plant Soil **218:** 185-196

Bradbury PJ, Zhang Z, Kroon DE, Casstevens TM, Ramdoss Y, Buckler ES (2007) TASSEL: software for association mapping of complex traits in diverse samples. Bioinformatics **23:** 2633-2635

Chen X, Goodwin SM, Boroff VL, Liu X, Jenks MA (2003) Cloning and characterization of the WAX2 gene of Arabidopsis involved in cuticle membrane and wax production.Plant Cell **15:** 1170-1185

Chimungu JG, Brown KM, Lynch JP (2014) Reduced root cortical cell file number improves drought tolerance in maize. Plant Physiol **166:** 1943-1955

Coudert Y, Périn C, Courtois B, Khong NG, Gantet P (2010) Genetic control of root development in rice, the model cereal. Trends Plant Sci **15:** 219-226

Courtois B, Ahmadi N, Khowaja F, Price AH, Rami J-F, Frouin J, Hamelin C, Ruiz M (2009) Rice root genetic architecture: Meta-analysis from a drought QTL database. Rice **2:** 115-128

Courtois B, Audebert A, Dardou A, Roques S, Ghneim- Herrera T, Droc G, Frouin J, Rouan L, Gozé E, Kilian A, Ahmadi N, Dingkuhn M (2013) Genome-wide association mapping of root traits in a japonica rice panel. PLoS ONE **8:** e78037

Crowell S, Korniliev P, Falcao A, Ismail A, Gregorio G, Mezey J, McCouch S (2016) Genome-wide association and high-resolution phenotyping link *Oryza sativa* panicle traits to numerous trait-specific QTL clusters. Nat Commun **7:** 10527

Dimkpa SON, Lahari Z, Shrestha R, Douglas A, Gheysen G, Price AH (2016) A genome-wide association study of a global rice panel reveals resistance in *Oryza sativ*a to root-knot nematodes. J Exp Bot **67:** 1191-1200

Duitama J, Quintero JC, Cruz DF, Quintero C, Hubmann G, Foulquié-Moreno MR, Verstrepen KJ, Thevelein JM, Tohme J (2014) An integrated framework for discovery and genotyping of genomic variants from high-throughput sequencing experiments. Nucleic Acids Res **42:** e44-e44

Elshire RJ, Glaubitz JC, Sun Q, Poland JA, Kawamoto K, Buckler ES, Mitchell SE (2011) A robust, simple genotyping-by-sequencing (GBS) approach for high diversity species. PLoS ONE **6:** e19379

Flexas J, Ribas-Carbó M, Hanson DT, Bota J, Otto B, Cifre J, McDowell N, Medrano H, Kaldenhoff R (2006) Tobacco aquaporin NtAQP1 is involved in mesophyll conductance to CO_2 in vivo. Plant J **48:** 427-439

Gao M-j, Parkin I, Lydiate D, Hannoufa A (2004) An auxin-responsive SCARECROW-like transcriptional activator interacts with histone deacetylase. Plant Mol Bio **55:** 417-431

Grieneisen VA, Xu J, Maree AFM, Hogeweg P, Scheres B (2007) Auxin transport is sufficient to generate a maximum and gradient guiding root growth. Nature **449:** 1008-1013

Hawker NP, Bowman JL (2004) Roles for class III HD-Zip and KANADI genes in Arabidopsis root development. Plant Physiol **135:** 2261-2270

Henry A, Cal AJ, Batoto TC, Torres RO, Serraj R (2012) Root attributes affecting water uptake of rice (*Oryza sativa*) under drought. J Exp Bot **63:** 4751-4763

Huang X, Wei X, Sang T, Zhao Q, Feng Q, Zhao Y, Li C, Zhu C, Lu T, Zhang Z, Li M, Fan D, Guo Y, Wang A, Wang L, Deng L, Li W, Lu Y, Weng Q, Liu K, Huang T, Zhou T, Jing Y, Li W, Lin Z, Buckler ES, Qian Q, Zhang Q-F, Li J, Han B (2010) Genome-wide association studies of 14 agronomic traits in rice landraces. Nat Genet **42:** 961-967

Ingvarsson PK, Street NR (2011) Association genetics of complex traits in plants. New Phytol **189:** 909-922

Jansen RC, Stam P (1994) High resolution of quantitative traits into multiple loci via interval mapping. Genetics **136:** 1447-1455

Juenger TE (2013) Natural variation and genetic constraints on drought tolerance. Curr Opin Plant Biol **16:** 274-281

Kadam N, Yin X, Bindraban P, Struik P, Jagadish K (2015) Does morphological and anatomical plasticity during the vegetative stage make wheat more tolerant of water-deficit stress than rice? Plant Physiol **167:** 1389-1401

Kawahara Y, de la Bastide M, Hamilton JP, Kanamori H, McCombie WR, Ouyang S, Schwartz DC, Tanaka T, Wu J, Zhou S, Childs KL, Davidson RM, Lin H, Quesada-Ocampo L, Vaillancourt B, Sakai H, Lee SS, Kim J, Numa H, Itoh T, Buell CR, Matsumoto T (2013) Improvement of the *Oryza sativa* nipponbare reference genome using next generation sequence and optical map data. Rice **6:** 4

Kikuchi S, Bheemanahalli R, Jagadish KSV, Kumagai E, Masuya Y, Kuroda E, Raghavan C, Dingkuhn M, Abe A, Shimono HCPCER (2017) Genome-wide association mapping for phenotypic plasticity in rice. Plant Cell Environ**:** DOI: 10.1111/pce.12955

Kumar A, Dixit S, Ram T, Yadaw RB, Mishra KK, Mandal NP (2014) Breeding high-yielding drought-tolerant rice: genetic variations and conventional and molecular approaches. J Exp Bot **65:** 6265-6278

Lipka AE, Tian F, Wang Q, Peiffer J, Li M, Bradbury PJ, Gore MA, Buckler ES, Zhang Z (2012) GAPIT: genome association and prediction integrated tool. Bioinformatics **28:** 2397-2399

Mackay I, Powell W (2007) Methods for linkage disequilibrium mapping in crops. Trends Plant Sci **12:** 57-63

Markakis MN, Boron AK, Van Loock B, Saini K, Cirera S, Verbelen J-P, Vissenberg K (2013) Characterization of a small auxinup RNA (SAUR)-like gene involved in *Arabidopsis thaliana* development. PLoS ONE **8:** e82596

Mather KA, Caicedo AL, Polato NR, Olsen KM, McCouch S, Purugganan MD (2007) The extent of linkage disequilibrium in rice (*Oryza sativa* L.). Genetics **177:** 2223

McCouch S, Baute GJ, Bradeen J, Bramel P, Bretting PK, Buckler E, Burke JM, Charest D, Cloutier S, Cole G, Dempewolf H, Dingkuhn M, Feuillet C, Gepts P, Grattapaglia D, Guarino L, Jackson S, Knapp S, Langridge P, Lawton-Rauh A,

Lijua Q, Lusty C, Michael T, Myles S, Naito K, Nelson RL, Pontarollo R, Richards CM, Rieseberg L, Ross-Ibarra J, Rounsley S, Hamilton RS, Schurr U, Stein N, Tomooka N, van der Knaap E, van Tassel D, Toll J, Valls J, Varshney RK, Ward J, Waugh R, Wenzl P, Zamir D (2013) Agriculture: Feeding the future. Nature **499:** 23-24

Nahirñak V, Almasia NI, Hopp HE, Vazquez-Rovere C (2012) Snakin/GASA proteins: Involvement in hormone crosstalk and redox homeostasis. Plant Signal Behav **7:** 1004-1008

Nicotra AB, Atkin OK, Bonser SP, Davidson AM, Finnegan EJ, Mathesius U, Poot P, Purugganan MD, Richards CL, Valladares F, van Kleunen M (2010) Plant phenotypic plasticity in a changing climate. Trends in Plant Science **15:** 684-692

Nicotra AB, Davidson A (2010) Adaptive phenotypic plasticity and plant water use. Funct Plant Biol **37:** 117-127

Norton GJ, Douglas A, Lahner B, Yakubova E, Guerinot ML, Pinson SRM, Tarpley L, Eizenga GC, McGrath SP, Zhao F-J, Islam MR, Islam S, Duan G, Zhu Y, Salt DE, Meharg AA, Price AH (2014) Genome wide association mapping of grain arsenic, copper, molybdenum and zinc in rice (*Oryza sativa* L.) grown at four international field sites. PLoS ONE **9:** e89685

Ohashi-Ito K, Oguchi M, Kojima M, Sakakibara H, Fukuda H (2013) Auxin-associated initiation of vascular cell differentiation by LONESOME HIGHWAY. Development **140:** 765-769

Phung NTP, Mai CD, Hoang GT, Truong HTM, Lavarenne J, Gonin M, Nguyen KL, Ha TT, Do VN, Gantet P, Courtois B (2016) Genome-wide association mapping for root traits in a panel of rice accessions from Vietnam. BMC Plant Biol **16:** 64

Poorter H, Bühler J, van Dusschoten D, Climent J, Postma JA (2012) Pot size matters: a meta-analysis of the effects of rooting volume on plant growth. Funct Plant Biol **39:** 839-850

Premachandra GS, Hahn DT, Axtell JD, Joly RJ (1994) Epicuticular wax load and water-use efficiency in bloomless and sparse-bloom mutants of Sorghum bicolor L. Environ Exper Bot **34:** 293-301

Qi W, Sun F, Wang Q, Chen M, Huang Y, Feng Y-Q, Luo X, Yang J (2011) Rice ethylene-response AP2/ERF factor OsEATB restricts internode elongation by down-regulating a gibberellin biosynthetic gene. Plant Physiol **157:** 216-228

Rebolledo MC, Peña AL, Duitama J, Cruz DF, Dingkuhn M, Grenier C, Tohme J (2016) Combining image analysis, genome wide association studies and different field trials to reveal stable genetic regions related to panicle architecture and the number of spikelets per panicle in rice. Front Plant Sci **7:** 1384

Rosegrant MW, Ringler C, Sulser TB, Ewing M, Palazzo A, Zhu T, Nelson GC, Koo J, RObertson R, Msangi S, Batka M (2009). Agriculture and food security under global change: Prospects for 2025/2050. *Background note for supporting the development of CGIAR Strategy and Results Framework. International Food Policy Research Institute: Washington, DC*.

Sambatti JBM, Caylor KK (2007) When is breeding for drought tolerance optimal if drought is random? New Phytol **175:** 70-80

Sandhu N, Raman KA, Torres RO, Audebert A, Dardou A, Kumar A, Henry A (2016) Rice root architectural plasticity traits and genetic regions for adaptability to variable cultivation and stress conditions. Plant Physiology **171:** 2562-2576

Sandhu N, Singh A, Dixit S, Sta Cruz MT, Maturan PC, Jain RK, Kumar A (2014) Identification and mapping of stable QTL with main and epistasis effect on rice grain yield under upland drought stress. BMC Genet **15:** 1-15

Scheet P, Stephens M (2006) A fast and flexible statistical model for large-scale population genotype data: applications to inferring missing genotypes and haplotypic phase. Am J Hum Genet **78:** 629-644

Schneider CA, Rasband WS, Eliceiri KW (2012) NIH Image to ImageJ: 25 years of image analysis. Nat Methods **9:** 671-675

Segura V, Vilhjalmsson BJ, Platt A, Korte A, Seren U, Long Q, Nordborg M (2012) An efficient multi-locus mixed-model approach for genome-wide association studies in structured populations. Nat Genet **44:** 825-830

Uga Y, Okuno K, Yano M (2008) QTLs underlying natural variation in stele and xylem structures of rice root. Breed Sci **58:** 7-14

Uga Y, Sugimoto K, Ogawa S, Rane J, Ishitani M, Hara N, Kitomi Y, Inukai Y, Ono K, Kanno N, Inoue H, Takehisa H, Motoyama R, Nagamura Y, Wu J, Matsumoto T, Takai T, Okuno K, Yano M (2013) Control of root system architecture by DEEPER ROOTING 1 increases rice yield under drought conditions. Nat Genet **45:** 1097-1102

Vejchasarn P, Lynch JP, Brown KM (2016) Genetic Variability in Phosphorus Responses of Rice Root Phenotypes. Rice **9:** 29

Yin X, Chasalow SD, Stam P, Kropff MJ, Dourleijn CJ, Bos I, Bindraban PS (2002) Use of component analysis in QTL mapping of complex crop traits: a case study on yield in barley. Plant Breed **121:** 314-319

Yoshida S, Hasegawa S (1982) The rice root system: its development and function. *Drought resistance in crops with emphasis on rice, International Rice Research Institute, Manila* **10:** 97-134

Zhang Z, Ersoz E, Lai C-Q, Todhunter RJ, Tiwari HK, Gore MA, Bradbury PJ, Yu J, Arnett DK, Ordovas JM, Buckler ES (2010) Mixed linear model approach adapted for genome-wide association studies. Nat Genet **42:** 355-360

Zhao C, Craig JC, Petzold HE, Dickerman AW, Beers EP (2005) The xylem and phloem transcriptomes from secondary tissues of the Arabidopsis root-hypocotyl. Plant Physiol **138:** 803-818

Zhao K, Tung C-W, Eizenga GC, Wright MH, Ali ML, Price AH, Norton GJ, Islam MR, Reynolds A, Mezey J, McClung AM, Bustamante CD, McCouch SR (2011) Genome-wide association mapping reveals a rich genetic architecture of complex traits in *Oryza sativa*. Nat Commun **2:** 467

Table 1. The list of measured and derived phenotypic traits broadly classified into five categories (A-E) with trait acronyms and units.

Traits	Trait acronym	Unit	Phenotypic plasticity acronym
(A) Shoot morphological traits			
Plant height	PHT	cm	rPHT
Tiller number	TN	plant^{-1}	rTN
Total leaf area	TLA	m^2 plant^{-1}	rTLA
Specific leaf area	SLA	m^2 g^{-1}	rSLA
(B) Physiological traits			
Cumulative water transpiration	CWT	kg plant^{-1}	rCWT
Water use efficiency	WUE	g kg^{-1}	rWUE
(C) Root morphological traits			
Total root length	TRL	m plant^{-1}	rTRL
Root length (RL) with diameter (mm) class			
RL_0-0.5	RL005	m plant^{-1}	rRL005
RL_0.5-1.0	RL0510	m plant^{-1}	rRL0510
RL_1.0-1.5	RL1015	m plant^{-1}	rRL1015
RL_1.5-2.0	RL1520	m plant^{-1}	rRL1520
RL_2.0-2.5	RL2025	m plant^{-1}	rRL2025
RL_2.5-3.0	RL2530	m plant^{-1}	rRL2530
RL_3.0-3.5	RL3035	m plant^{-1}	rRL3035
RL_3.5	RL35	m plant^{-1}	rRL35
Maximum root length	MRL	cm	rMRL
Surface area	SA	cm^2 plant^{-1}	rSA
Root volume	RV	cm^3 plant^{-1}	rRV
Average root thickness	ART	mm	rART
Specific root length	SRL	m g^{-1}	rSRL
Total root weight density	TRWD	g cm^{-3}	rTRWD
Root length per unit leaf area	RLLA	m m^{-2}	rRLLA
(D) Root anatomical traits			
Root diameter	RD	µm	rRD
Cortex diameter	CD	µm	rCD
Stele diameter	SD	µm	rSD
Late metaxylem diameter	LMXD	µm	rLMXD
Late metaxylem number	LMXN	µm	rLMXN
Stele diameter in proportion of root diameter	SD:RD	%	rSDRD
(E) Dry matter traits			
Leaf weight	LW	g plant^{-1}	rLW
Stem weight	SW	g plant^{-1}	rSW
Root weight	RW	g plant^{-1}	rRW
Total weight	TW	g plant^{-1}	rTW
Root: shoot ratio	RS	-	rRS
Leaf weight ratio	LWR	-	rLWR
Stem weight ratio	SWR	-	rSWR

Table 2. Summary of significant loci identified by GWAS analysis using two approaches (comprised mixed linear model (CMLM) and multi-locus mixed model (MLMM) for 35 traits across five categories (A-E) in control (C) and water-deficit (WD) conditions and for phenotypic plasticity (PP) of traits as a relative measure.

Trait classification	**C**	**WD**	**PP**
(A) Shoot morphological traits	6	11	8
(B) Physiological traits	16	6	6
(C) Root morphological traits	34	52	33
(D) Root anatomical traits	14	17	15
(E) Dry matter traits	34	20	14
Total loci	**104 (22)**	**106 (10)**	**76 (9)**
Loci detected by CMLM approach	**39 [32%]**	**26 [24%]**	**19 [25%]**
Loci detected by MLMM approach	**42 [40%]**	**45 [42%]**	**36 [47%]**
Loci detected by both approaches	**23 [22%]**	**35 [33%]**	**21 [27%]**
Total predicted *a priori* genes	**296**	**284**	**233**
Genes responsive to abiotic stress stimulus	**48**	**61**	**38**

The values in parenthesis are loci associated with more than one trait (see **Supplementary Table S6**) and values in square brackets are the percentages of loci out of total loci detected by CMLM, MLMM and both the approaches. The total *a priori* genes are predicted in expected LD block of peak SNP/SNPs.

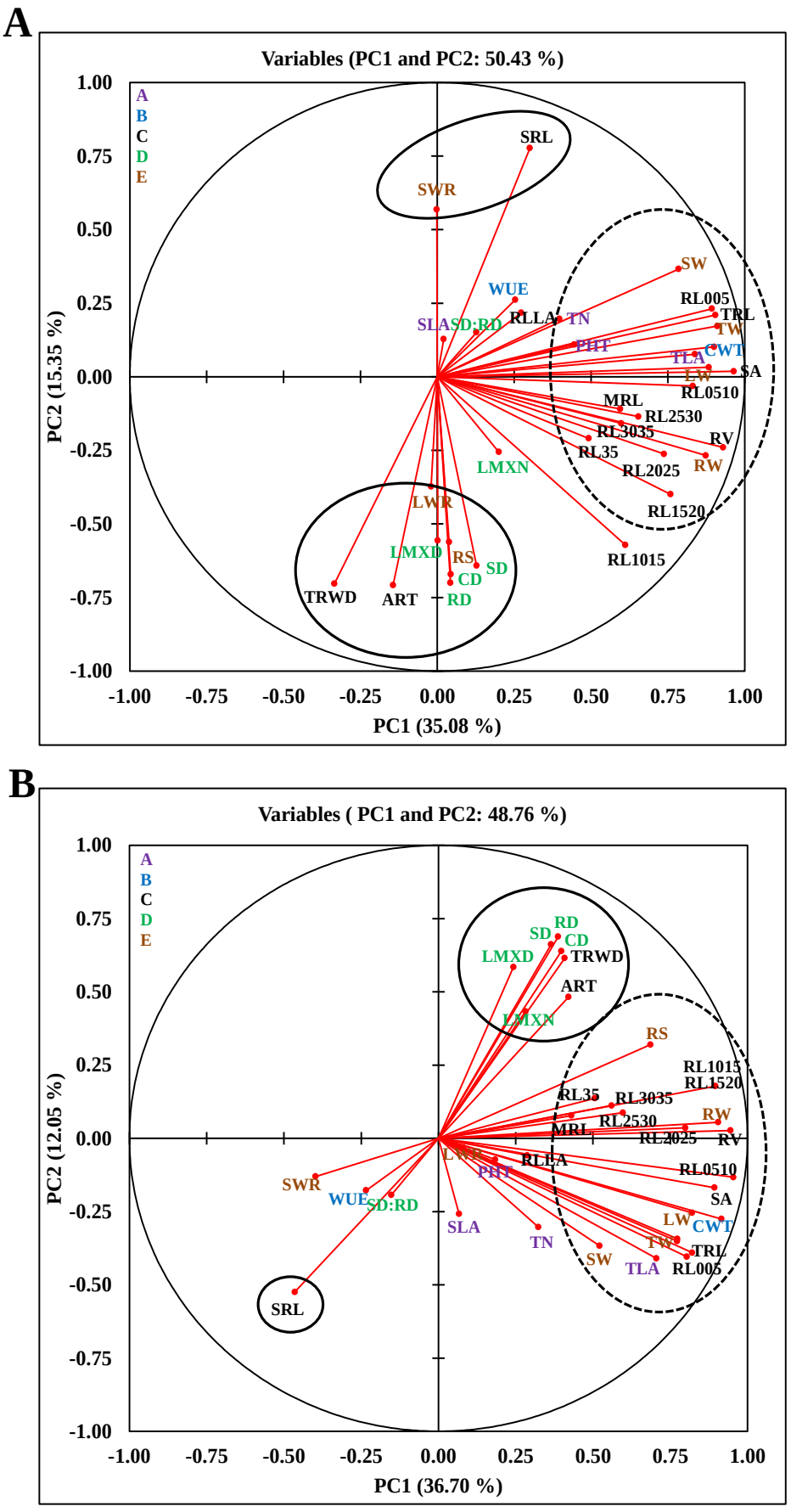

Figure 1. Principal component analysis of the 35 traits with first two components showing variation in control **(Panel A),** and water-deficit stress **(Panel B)** conditions. The traits marked by dashed ellipses contributing more to the variation explained by the PC1 and marked by solid circle/ellipses to PC2. Trait labels coloured differently according to category (uppercase letter in each panel) in Table 1; acronyms are given in the Table 1 as well.

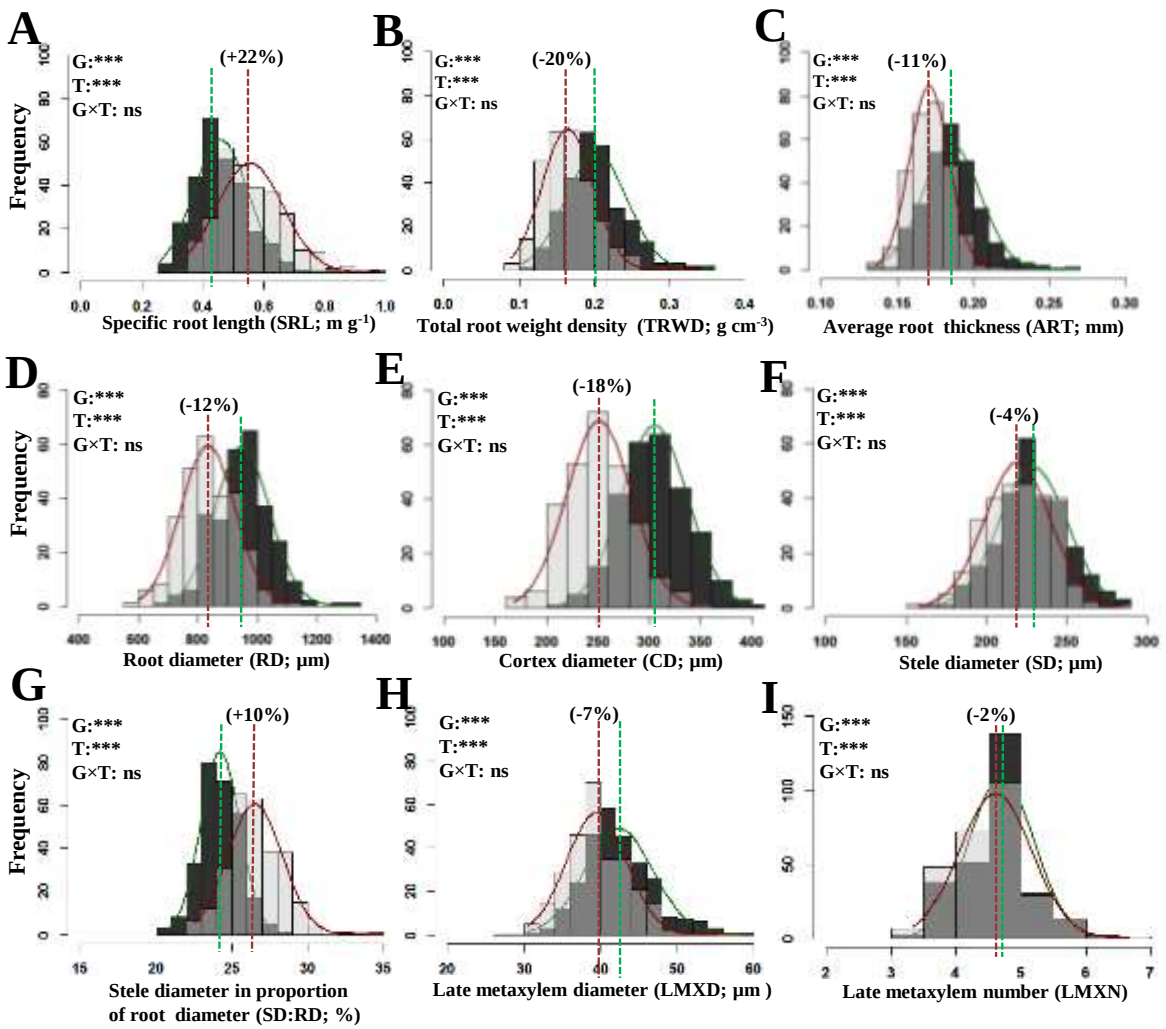

Figure 2. Overlying histograms with normal distribution curves (control: green line, dark grey bars; water-deficit stress: red line, light grey bars; intermediate grey: overlap for the treatment with the lower frequency value) showing the phenotypic distribution of root morphological **(Panel A-C)** and anatomical **(Panel D-I)** traits. The vertical lines in the histograms show population mean values in control (green) and water-deficit stress (red) conditions and values in parentheses represent the significant percentage change (+: increase or –: decrease) in water-deficit stress conditions over the control. Levels of significance for Genotype (G), Treatment (T) and their interaction (G×T) effects from ANOVA are given in the histograms (***, P<0.001; ns, not significant).

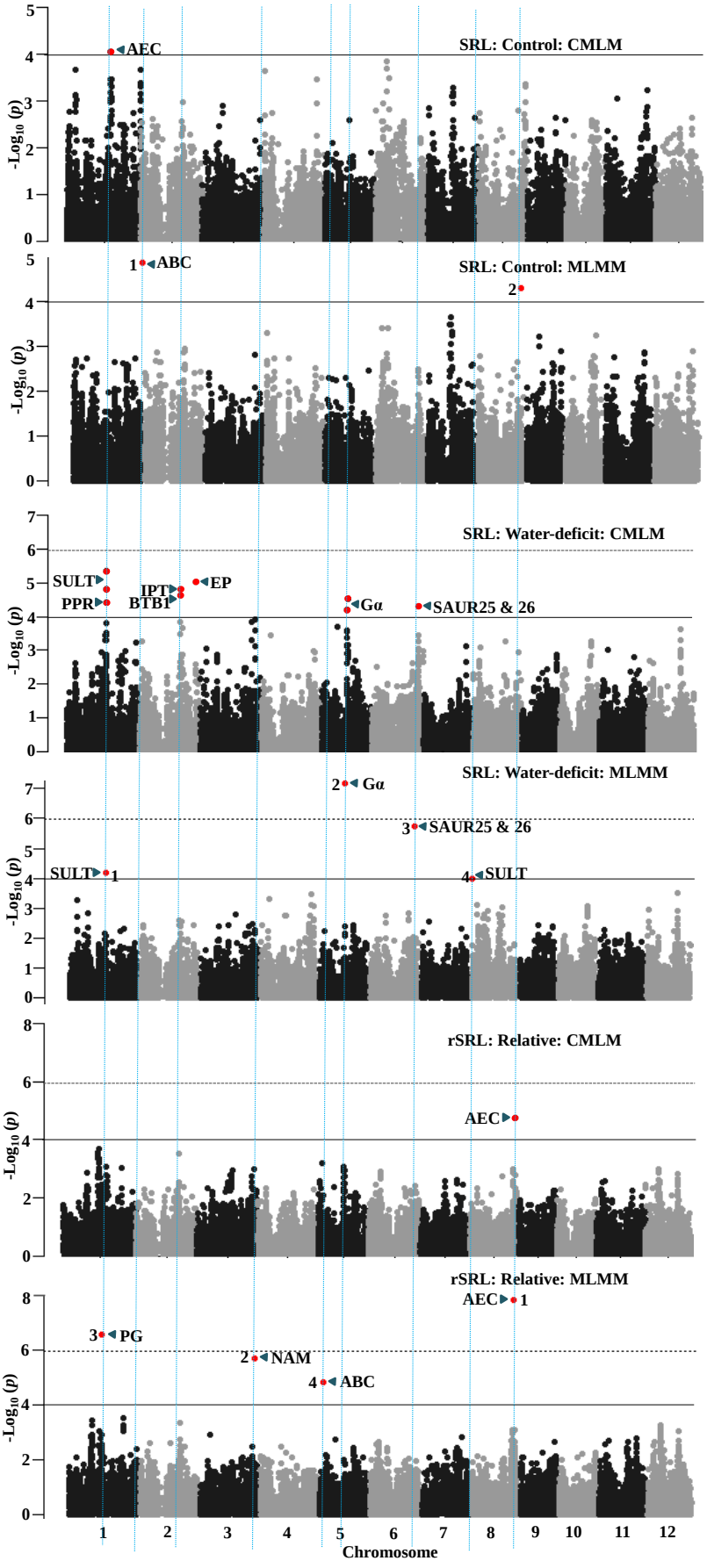

Figure 3. GWAS results through the compressed mixed linear model (CMLM) and the multi-locus mixed model (MLMM) approaches for specific root length (SRL) in control (the two upper panels) and water-deficit conditions (the two middle panels) and the trait plasticity calculated as the relative value of the water-deficit stress conditions over the control (the two bottom panels). Significant SNPs (coloured red in the Manhattan plots) are distinguished by

threshold *P* value lines (solid black= [$-\text{Log}_{10}$ *P* >4] and dotted black= Bonferroni-corrected threshold). Significant SNPs in MLMM Manhattan plots are numbered in the order that they were included in the model as a cofactor. *A priori* candidate genes (**Supplementary Tables S9-S11**) are indicated near to peak SNP/SNPs in the Manhattan plot. **AEC:** auxin efflux carrier; **ABC:** ATP-binding cassette transporters; **SULT:** Sulfate transporter; **PPR:** Pentatricopeptide; **IPT:** Inorganic phosphate transporter; **BTB1:** Brick-Brack, Tramtrack, Broad Complex BTB, **EP:** Expressed protein; **G*α*:** G-protein alpha subunit; **SAUR:** Small auxin UP-RNA; **PG:** Polygalacturonase; **NAM:** No apical meristem.

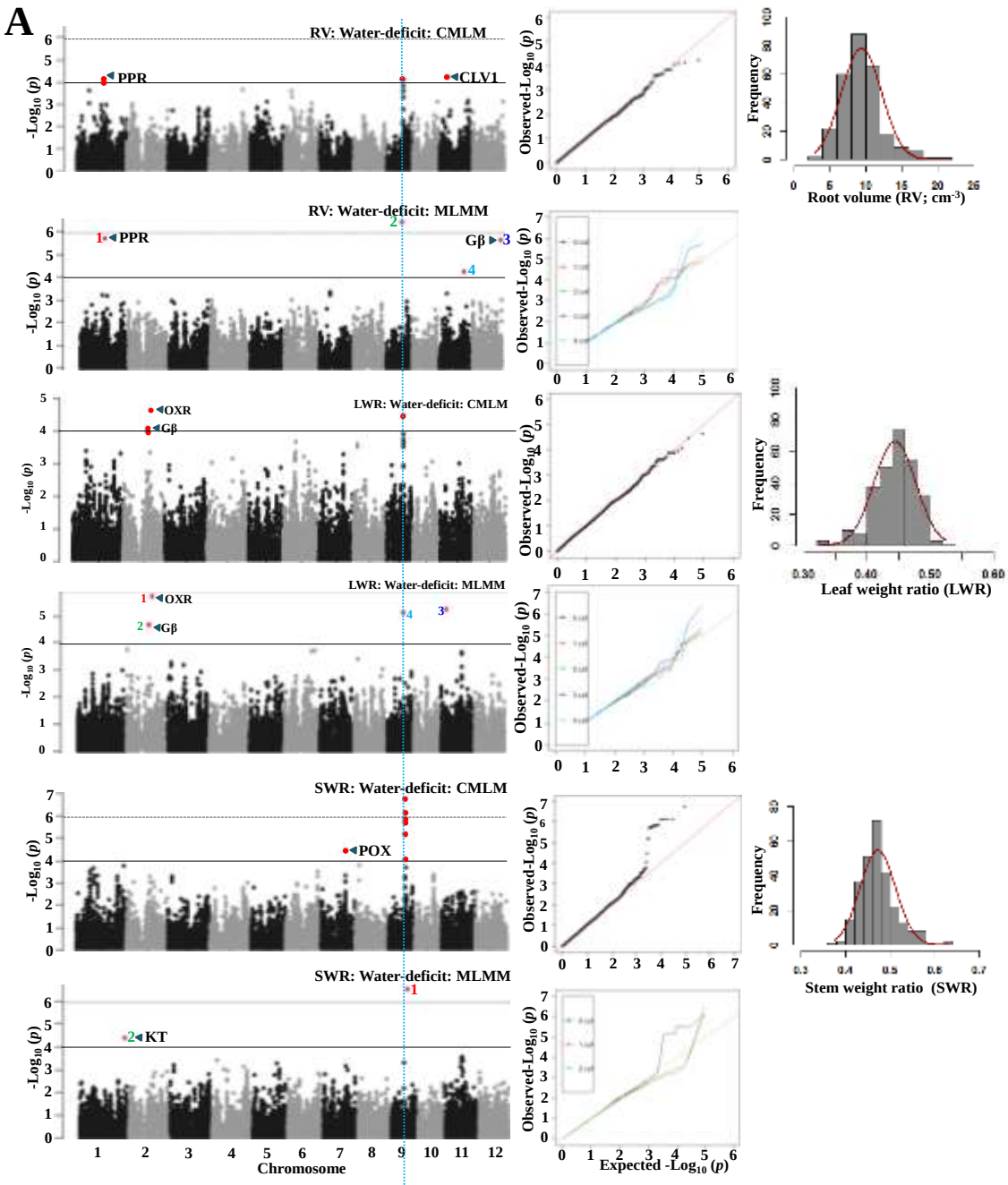

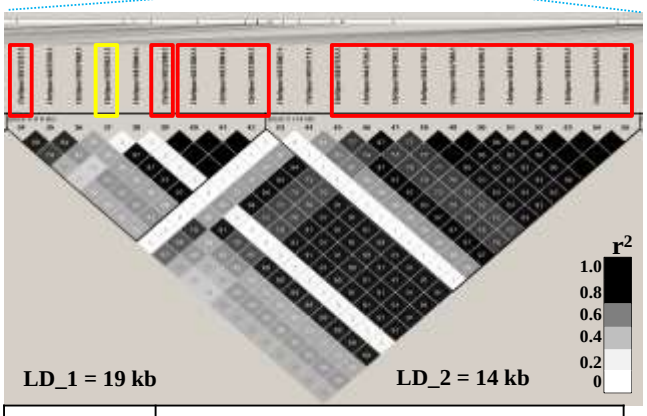

LD_1= 19 kb	GASA10-Gibberellin regulated protein
LD_2= 14 kb	GASA10-Gibberellin regulated protein

Figure 4. GWAS results through compressed mixed linear model (CMLM) and multi-locus mixed model (MLMM) approaches (Manhattan and Quantile-Quantile plots) for root volume (RV), leaf weight ratio (LWR) and stem weight ratio (SWR) in water-deficit stress.

Significant SNPs (coloured red in the Manhattan plots) are distinguished by threshold *P* value lines (solid black= [-Log_{10} *P* >4] and dotted black= Bonferroni-corrected significance threshold) and coloured red in the Manhattan plots (**Panel A**). Significant SNPs on MLMM Manhattan plots are numbered in the order that they were included in the model as a cofactor. Identified LD blocks based on pairwise r^2 values between SNPs on chromosome 9 (**Panel B**) with *a priori* candidate gene in the underneath table (for more details see **Supplementary Tables S8 and S10**). The colour intensity of the box corresponds with r^2 value (multiplied by 100) according to the legend. Significant SNP ("**14829621"**) marked in yellow rectangle was commonly associated with RV, LWR and SWR **(Panel B)**. **PPR:** Pentatricopeptide, **CLV1:** CLAVATA1; **Gβ:** G-protein beta subunit; **OXR:** Oxidoreductase; **POX:** Peroxidase; **KT:** Potassium transporter

Parsed Citations

Al-Tamimi N, Brien C, Oakey H, Berger B, Saade S, Ho YS, Schmöckel SM, Tester M, Negrão S (2016) Salinity tolerance loci revealed in rice using high-throughput non-invasive phenotyping. Nat Commun 7: 13342

Pubmed: Author and Title
CrossRef: Author and Title
Google Scholar: Author Only Title Only Author and Title

Barrett JC, Fry B, Maller J, Daly MJ (2005) Haploview: analysis and visualization of LD and haplotype maps. Bioinformatics 21: 263-265

Pubmed: Author and Title
CrossRef: Author and Title
Google Scholar: Author Only Title Only Author and Title

Bernier J, Serraj R, Kumar A, Venuprasad R, Impa S, R.P VG, Oane R, Spaner D, Atlin G (2009) The large-effect drought-resistance QTL qtl12.1 increases water uptake in upland rice. Field Crop Res 110: 139-146

Pubmed: Author and Title
CrossRef: Author and Title
Google Scholar: Author Only Title Only Author and Title

Biscarini F, Cozzi P, Casella L, Riccardi P, Vattari A, Orasen G, Perrini R, Tacconi G, Tondelli A, Biselli C, Cattivelli L, Spindel J, McCouch S, Abbruscato P, Valé G, Piffanelli P, Greco R (2016) Genome-wide association study for traits related to plant and grain morphology, and root architecture in temperate rice accessions. PLoS ONE 11: e0155425

Pubmed: Author and Title
CrossRef: Author and Title
Google Scholar: Author Only Title Only Author and Title

Bouma TJ, Nielsen KL, Koutstaal B (2000) Sample preparation and scanning protocol for computerised analysis of root length and diameter. Plant Soil 218: 185-196

Pubmed: Author and Title
CrossRef: Author and Title
Google Scholar: Author Only Title Only Author and Title

Bradbury PJ, Zhang Z, Kroon DE, Casstevens TM, Ramdoss Y, Buckler ES (2007) TASSEL: software for association mapping of complex traits in diverse samples. Bioinformatics 23: 2633-2635

Pubmed: Author and Title
CrossRef: Author and Title
Google Scholar: Author Only Title Only Author and Title

Chen X, Goodwin SM, Boroff VL, Liu X, Jenks MA (2003) Cloning and characterization of the WAX2 gene of Arabidopsis involved in cuticle membrane and wax production.Plant Cell 15: 1170-1185

Pubmed: Author and Title
CrossRef: Author and Title
Google Scholar: Author Only Title Only Author and Title

Chimungu JG, Brown KM, Lynch JP (2014) Reduced root cortical cell file number improves drought tolerance in maize. Plant Physiol 166: 1943-1955

Pubmed: Author and Title
CrossRef: Author and Title
Google Scholar: Author Only Title Only Author and Title

Coudert Y, Périn C, Courtois B, Khong NG, Gantet P (2010) Genetic control of root development in rice, the model cereal. Trends Plant Sci 15: 219-226

Pubmed: Author and Title
CrossRef: Author and Title
Google Scholar: Author Only Title Only Author and Title

Courtois B, Ahmadi N, Khowaja F, Price AH, Rami J-F, Frouin J, Hamelin C, Ruiz M (2009) Rice root genetic architecture: Meta-analysis from a drought QTL database. Rice 2: 115-128

Pubmed: Author and Title
CrossRef: Author and Title
Google Scholar: Author Only Title Only Author and Title

Courtois B, Audebert A, Dardou A, Roques S, Ghneim- Herrera T, Droc G, Frouin J, Rouan L, Gozé E, Kilian A, Ahmadi N, Dingkuhn M (2013) Genome-wide association mapping of root traits in a japonica rice panel. PLoS ONE 8: e78037

Pubmed: Author and Title
CrossRef: Author and Title
Google Scholar: Author Only Title Only Author and Title

Crowell S, Korniliev P, Falcao A, Ismail A, Gregorio G, Mezey J, McCouch S (2016) Genome-wide association and high-resolution phenotyping link Oryza sativa panicle traits to numerous trait-specific QTL clusters. Nat Commun 7: 10527

Pubmed: Author and Title
CrossRef: Author and Title
Google Scholar: Author Only Title Only Author and Title

Dimkpa SON, Lahari Z, Shrestha R, Douglas A, Gheysen G, Price AH (2016) A genome-wide association study of a global rice panel reveals resistance in Oryza sativa to root-knot nematodes. J Exp Bot 67: 1191-1200

Pubmed: Author and Title
CrossRef: Author and Title

Google Scholar: Author Only Title Only Author and Title

Duitama J, Quintero JC, Cruz DF, Quintero C, Hubmann G, Foulquié-Moreno MR, Verstrepen KJ, Thevelein JM, Tohme J (2014) An integrated framework for discovery and genotyping of genomic variants from high-throughput sequencing experiments. Nucleic Acids Res 42: e44-e44
Pubmed: Author and Title
CrossRef: Author and Title
Google Scholar: Author Only Title Only Author and Title

Elshire RJ, Glaubitz JC, Sun Q, Poland JA, Kawamoto K, Buckler ES, Mitchell SE (2011) A robust, simple genotyping-by-sequencing (GBS) approach for high diversity species. PLoS ONE 6: e19379
Pubmed: Author and Title
CrossRef: Author and Title
Google Scholar: Author Only Title Only Author and Title

Flexas J, Ribas-Carbó M, Hanson DT, Bota J, Otto B, Cifre J, McDowell N, Medrano H, Kaldenhoff R (2006) Tobacco aquaporin NtAQP1 is involved in mesophyll conductance to CO2 in vivo. Plant J 48: 427-439
Pubmed: Author and Title
CrossRef: Author and Title
Google Scholar: Author Only Title Only Author and Title

Gao M-j, Parkin I, Lydiate D, Hannoufa A (2004) An auxin-responsive SCARECROW-like transcriptional activator interacts with histone deacetylase. Plant Mol Bio 55: 417-431
Pubmed: Author and Title
CrossRef: Author and Title
Google Scholar: Author Only Title Only Author and Title

Grieneisen VA, Xu J, Maree AFM, Hogeweg P, Scheres B (2007) Auxin transport is sufficient to generate a maximum and gradient guiding root growth. Nature 449: 1008-1013
Pubmed: Author and Title
CrossRef: Author and Title
Google Scholar: Author Only Title Only Author and Title

Hawker NP, Bowman JL (2004) Roles for class III HD-Zip and KANADI genes in Arabidopsis root development. Plant Physiol 135: 2261-2270
Pubmed: Author and Title
CrossRef: Author and Title
Google Scholar: Author Only Title Only Author and Title

Henry A, Cal AJ, Batoto TC, Torres RO, Serraj R (2012) Root attributes affecting water uptake of rice (Oryza sativa) under drought. J Exp Bot 63: 4751-4763
Pubmed: Author and Title
CrossRef: Author and Title
Google Scholar: Author Only Title Only Author and Title

Huang X, Wei X, Sang T, Zhao Q, Feng Q, Zhao Y, Li C, Zhu C, Lu T, Zhang Z, Li M, Fan D, Guo Y, Wang A, Wang L, Deng L, Li W, Lu Y, Weng Q, Liu K, Huang T, Zhou T, Jing Y, Li W, Lin Z, Buckler ES, Qian Q, Zhang Q-F, Li J, Han B (2010) Genome-wide association studies of 14 agronomic traits in rice landraces. Nat Genet 42: 961-967
Pubmed: Author and Title
CrossRef: Author and Title
Google Scholar: Author Only Title Only Author and Title

Ingvarsson PK, Street NR (2011) Association genetics of complex traits in plants. New Phytol 189: 909-922
Pubmed: Author and Title
CrossRef: Author and Title
Google Scholar: Author Only Title Only Author and Title

Jansen RC, Stam P (1994) High resolution of quantitative traits into multiple loci via interval mapping. Genetics 136: 1447-1455
Pubmed: Author and Title
CrossRef: Author and Title
Google Scholar: Author Only Title Only Author and Title

Juenger TE (2013) Natural variation and genetic constraints on drought tolerance. Curr Opin Plant Biol 16: 274-281
Pubmed: Author and Title
CrossRef: Author and Title
Google Scholar: Author Only Title Only Author and Title

Kadam N, Yin X, Bindraban P, Struik P, Jagadish K (2015) Does morphological and anatomical plasticity during the vegetative stage make wheat more tolerant of water-deficit stress than rice? Plant Physiol 167: 1389-1401
Pubmed: Author and Title
CrossRef: Author and Title
Google Scholar: Author Only Title Only Author and Title

Kawahara Y, de la Bastide M, Hamilton JP, Kanamori H, McCombie WR, Ouyang S, Schwartz DC, Tanaka T, Wu J, Zhou S, Childs KL, Davidson RM, Lin H, Quesada-Ocampo L, Vaillancourt B, Sakai H, Lee SS, Kim J, Numa H, Itoh T, Buell CR, Matsumoto T (2013) Improvement of the Oryza sativa nipponbare reference genome using next generation sequence and optical map data. Rice 6: 4
Pubmed: Author and Title
CrossRef: Author and Title
Google Scholar: Author Only Title Only Author and Title

Kikuchi S, Bheemanahalli R, Jagadish KSV, Kumagai E, Masuya Y, Kuroda E, Raghavan C, Dingkuhn M, Abe A, Shimono HCPCER

(2017) Genome-wide association mapping for phenotypic plasticity in rice. Plant Cell Environ: DOI: 10.1111/pce.12955
Pubmed: Author and Title
CrossRef: Author and Title
Google Scholar: Author Only Title Only Author and Title

Kumar A, Dixit S, Ram T, Yadaw RB, Mishra KK, Mandal NP (2014) Breeding high-yielding drought-tolerant rice: genetic variations and conventional and molecular approaches. J Exp Bot 65: 6265-6278
Pubmed: Author and Title
CrossRef: Author and Title
Google Scholar: Author Only Title Only Author and Title

Lipka AE, Tian F, Wang Q, Peiffer J, Li M, Bradbury PJ, Gore MA, Buckler ES, Zhang Z (2012) GAPIT: genome association and prediction integrated tool. Bioinformatics 28: 2397-2399
Pubmed: Author and Title
CrossRef: Author and Title
Google Scholar: Author Only Title Only Author and Title

Mackay I, Powell W (2007) Methods for linkage disequilibrium mapping in crops. Trends Plant Sci 12: 57-63
Pubmed: Author and Title
CrossRef: Author and Title
Google Scholar: Author Only Title Only Author and Title

Markakis MN, Boron AK, Van Loock B, Saini K, Cirera S, Verbelen J-P, Vissenberg K (2013) Characterization of a small auxinup RNA (SAUR)-like gene involved in Arabidopsis thaliana development. PLoS ONE 8: e82596
Pubmed: Author and Title
CrossRef: Author and Title
Google Scholar: Author Only Title Only Author and Title

Mather KA, Caicedo AL, Polato NR, Olsen KM, McCouch S, Purugganan MD (2007) The extent of linkage disequilibrium in rice (Oryza sativa L.). Genetics 177: 2223
Pubmed: Author and Title
CrossRef: Author and Title
Google Scholar: Author Only Title Only Author and Title

McCouch S, Baute GJ, Bradeen J, Bramel P, Bretting PK, Buckler E, Burke JM, Charest D, Cloutier S, Cole G, Dempewolf H, Dingkuhn M, Feuillet C, Gepts P, Grattapaglia D, Guarino L, Jackson S, Knapp S, Langridge P, Lawton-Rauh A, Lijua Q, Lusty C, Michael T, Myles S, Naito K, Nelson RL, Pontarollo R, Richards CM, Rieseberg L, Ross-Ibarra J, Rounsley S, Hamilton RS, Schurr U, Stein N, Tomooka N, van der Knaap E, van Tassel D, Toll J, Valls J, Varshney RK, Ward J, Waugh R, Wenzl P, Zamir D (2013) Agriculture: Feeding the future. Nature 499: 23-24
Pubmed: Author and Title
CrossRef: Author and Title
Google Scholar: Author Only Title Only Author and Title

Nahirñak V, Almasia NI, Hopp HE, Vazquez-Rovere C (2012) Snakin/GASA proteins: Involvement in hormone crosstalk and redox homeostasis. Plant Signal Behav 7: 1004-1008
Pubmed: Author and Title
CrossRef: Author and Title
Google Scholar: Author Only Title Only Author and Title

Nicotra AB, Atkin OK, Bonser SP, Davidson AM, Finnegan EJ, Mathesius U, Poot P, Purugganan MD, Richards CL, Valladares F, van Kleunen M (2010) Plant phenotypic plasticity in a changing climate. Trends in Plant Science 15: 684-692
Pubmed: Author and Title
CrossRef: Author and Title
Google Scholar: Author Only Title Only Author and Title

Nicotra AB, Davidson A (2010) Adaptive phenotypic plasticity and plant water use. Funct Plant Biol 37: 117-127
Pubmed: Author and Title
CrossRef: Author and Title
Google Scholar: Author Only Title Only Author and Title

Norton GJ, Douglas A, Lahner B, Yakubova E, Guerinot ML, Pinson SRM, Tarpley L, Eizenga GC, McGrath SP, Zhao F-J, Islam MR, Islam S, Duan G, Zhu Y, Salt DE, Meharg AA, Price AH (2014) Genome wide association mapping of grain arsenic, copper, molybdenum and zinc in rice (Oryza sativa L.) grown at four international field sites. PLoS ONE 9: e89685
Pubmed: Author and Title
CrossRef: Author and Title
Google Scholar: Author Only Title Only Author and Title

Ohashi-Ito K, Oguchi M, Kojima M, Sakakibara H, Fukuda H (2013) Auxin-associated initiation of vascular cell differentiation by LONESOME HIGHWAY. Development 140: 765-769
Pubmed: Author and Title
CrossRef: Author and Title
Google Scholar: Author Only Title Only Author and Title

Phung NTP, Mai CD, Hoang GT, Truong HTM, Lavarenne J, Gonin M, Nguyen KL, Ha TT, Do VN, Gantet P, Courtois B (2016) Genome-wide association mapping for root traits in a panel of rice accessions from Vietnam. BMC Plant Biol 16: 64
Pubmed: Author and Title
CrossRef: Author and Title
Google Scholar: Author Only Title Only Author and Title

Poorter H, Bühler J, van Dusschoten D, Climent J, Postma JA (2012) Pot size matters: a meta-analysis of the effects of rooting

volume on plant growth. Funct Plant Biol 39: 839-850
Pubmed: Author and Title
CrossRef: Author and Title
Google Scholar: Author Only Title Only Author and Title

Premachandra GS, Hahn DT, Axtell JD, Joly RJ (1994) Epicuticular wax load and water-use efficiency in bloomless and sparse-bloom mutants of Sorghum bicolor L. Environ Exper Bot 34: 293-301
Pubmed: Author and Title
CrossRef: Author and Title
Google Scholar: Author Only Title Only Author and Title

Qi W, Sun F, Wang Q, Chen M, Huang Y, Feng Y-Q, Luo X, Yang J (2011) Rice ethylene-response AP2/ERF factor OsEATB restricts internode elongation by down-regulating a gibberellin biosynthetic gene. Plant Physiol 157: 216-228
Pubmed: Author and Title
CrossRef: Author and Title
Google Scholar: Author Only Title Only Author and Title

Rebolledo MC, Peña AL, Duitama J, Cruz DF, Dingkuhn M, Grenier C, Tohme J (2016) Combining image analysis, genome wide association studies and different field trials to reveal stable genetic regions related to panicle architecture and the number of spikelets per panicle in rice. Front Plant Sci 7: 1384
Pubmed: Author and Title
CrossRef: Author and Title
Google Scholar: Author Only Title Only Author and Title

Rosegrant MW, Ringler C, Sulser TB, Ewing M, Palazzo A, Zhu T, Nelson GC, Koo J, RObertson R, Msangi S, Batka M (2009). Agriculture and food security under global change: Prospects for 2025/2050. Background note for supporting the development of CGIAR Strategy and Results Framework. International Food Policy Research Institute: Washington, DC.
Pubmed: Author and Title
CrossRef: Author and Title
Google Scholar: Author Only Title Only Author and Title

Sambatti JBM, Caylor KK (2007) When is breeding for drought tolerance optimal if drought is random? New Phytol 175: 70-80
Pubmed: Author and Title
CrossRef: Author and Title
Google Scholar: Author Only Title Only Author and Title

Sandhu N, Raman KA, Torres RO, Audebert A, Dardou A, Kumar A, Henry A (2016) Rice root architectural plasticity traits and genetic regions for adaptability to variable cultivation and stress conditions. Plant Physiology 171: 2562-2576
Pubmed: Author and Title
CrossRef: Author and Title
Google Scholar: Author Only Title Only Author and Title

Sandhu N, Singh A, Dixit S, Sta Cruz MT, Maturan PC, Jain RK, Kumar A (2014) Identification and mapping of stable QTL with main and epistasis effect on rice grain yield under upland drought stress. BMC Genet 15: 1-15
Pubmed: Author and Title
CrossRef: Author and Title
Google Scholar: Author Only Title Only Author and Title

Scheet P, Stephens M (2006) A fast and flexible statistical model for large-scale population genotype data: applications to inferring missing genotypes and haplotypic phase. Am J Hum Genet 78: 629-644
Pubmed: Author and Title
CrossRef: Author and Title
Google Scholar: Author Only Title Only Author and Title

Schneider CA, Rasband WS, Eliceiri KW (2012) NIH Image to ImageJ: 25 years of image analysis. Nat Methods 9: 671-675
Pubmed: Author and Title
CrossRef: Author and Title
Google Scholar: Author Only Title Only Author and Title

Segura V, Vilhjalmsson BJ, Platt A, Korte A, Seren U, Long Q, Nordborg M (2012) An efficient multi-locus mixed-model approach for genome-wide association studies in structured populations. Nat Genet 44: 825-830
Pubmed: Author and Title
CrossRef: Author and Title
Google Scholar: Author Only Title Only Author and Title

Uga Y, Okuno K, Yano M (2008) QTLs underlying natural variation in stele and xylem structures of rice root. Breed Sci 58: 7-14
Pubmed: Author and Title
CrossRef: Author and Title
Google Scholar: Author Only Title Only Author and Title

Uga Y, Sugimoto K, Ogawa S, Rane J, Ishitani M, Hara N, Kitomi Y, Inukai Y, Ono K, Kanno N, Inoue H, Takehisa H, Motoyama R, Nagamura Y, Wu J, Matsumoto T, Takai T, Okuno K, Yano M (2013) Control of root system architecture by DEEPER ROOTING 1 increases rice yield under drought conditions. Nat Genet 45: 1097-1102
Pubmed: Author and Title
CrossRef: Author and Title
Google Scholar: Author Only Title Only Author and Title

Vejchasarn P, Lynch JP, Brown KM (2016) Genetic Variability in Phosphorus Responses of Rice Root Phenotypes. Rice 9: 29
Pubmed: Author and Title
CrossRef: Author and Title
Google Scholar: Author Only Title Only Author and Title

Yin X, Chasalow SD, Stam P, Kropff MJ, Dourleijn CJ, Bos I, Bindraban PS (2002) Use of component analysis in QTL mapping of complex crop traits: a case study on yield in barley. Plant Breed 121: 314-319
Pubmed: Author and Title
CrossRef: Author and Title
Google Scholar: Author Only Title Only Author and Title

Yoshida S, Hasegawa S (1982) The rice root system: its development and function. Drought resistance in crops with emphasis on rice, International Rice Research Institute, Manila 10: 97-134
Pubmed: Author and Title
CrossRef: Author and Title
Google Scholar: Author Only Title Only Author and Title

Zhang Z, Ersoz E, Lai C-Q, Todhunter RJ, Tiwari HK, Gore MA, Bradbury PJ, Yu J, Arnett DK, Ordovas JM, Buckler ES (2010) Mixed linear model approach adapted for genome-wide association studies. Nat Genet 42: 355-360
Pubmed: Author and Title
CrossRef: Author and Title
Google Scholar: Author Only Title Only Author and Title

Zhao C, Craig JC, Petzold HE, Dickerman AW, Beers EP (2005) The xylem and phloem transcriptomes from secondary tissues of the Arabidopsis root-hypocotyl. Plant Physiol 138: 803-818
Pubmed: Author and Title
CrossRef: Author and Title
Google Scholar: Author Only Title Only Author and Title

Zhao K, Tung C-W, Eizenga GC, Wright MH, Ali ML, Price AH, Norton GJ, Islam MR, Reynolds A, Mezey J, McClung AM, Bustamante CD, McCouch SR (2011) Genome-wide association mapping reveals a rich genetic architecture of complex traits in Oryza sativa. Nat Commun 2: 467
Pubmed: Author and Title
CrossRef: Author and Title
Google Scholar: Author Only Title Only Author and Title